Pacific Northwest
NATIONAL LABORATORY

PNNL-30024, Rev. 0
RPT-OSIF-009, Rev. 0

# Transfer and Flushing Evaluation for Potential Precipitated Solids in the 241-AP-106 to EMF Transfer Pipeline for DFLAW

June 2020

BE Wells
LA Mahoney
MS Fountain

U.S. DEPARTMENT OF ENERGY

Prepared for the U.S. Department of Energy
under Contract DE-AC05-76RL01830

## DISCLAIMER



PACIFIC NORTHWEST NATIONAL LABORATORY
*operated by*
BATTELLE
*for the*
UNITED STATES DEPARTMENT OF ENERGY
*under Contract DE-AC05-76RL01830*

**Printed in the United States of America**

**Available to DOE and DOE contractors from the**
**Office of Scientific and Technical Information,**
**P.O. Box 62, Oak Ridge, TN 37831-0062;**
**ph: (865) 576-8401**
**fax: (865) 576-5728**
**email: reports@adonis.osti.gov**

**Available to the public from the National Technical Information Service**
**5301 Shawnee Rd., Alexandria, VA 22312**
**ph: (800) 553-NTIS (6847)**
**email: orders@ntis.gov <https://www.ntis.gov/about>**
**Online ordering: http://www.ntis.gov**

PNNL-30024, Rev. 0
RPT-OSIF-009, Rev. 0

# Transfer and Flushing Evaluation for Potential Precipitated Solids in the 241-AP-106 to EMF Transfer Pipeline for DFLAW

June 2020

BE Wells
LA Mahoney
MS Fountain

Prepared for
the U.S. Department of Energy
under Contract DE-AC05-76RL01830

Pacific Northwest National Laboratory
Richland, Washington 99354

# Summary

Sufficient waste transfer velocity and pipeline flushing capabilities are necessary to maintain pipeline performance. However, added flush fluid increases the nuclear waste inventory resulting in additional mission costs due to added 242-Evaporator campaigns and increased secondary liquid waste disposal. During the Direct Feed Low-Activity Waste (DFLAW) mission, waste transfer lines from the Interim Low-Activity Waste Storage Tank (i.e., 241-AP-106; hereafter AP-106) to the Hanford Waste Treatment and Immobilization Plant (WTP) Low-Activity Waste (LAW) Facility must have the capability of being flushed to prevent accumulation of solids and to mitigate corrosion concerns.

Operational experience at Hanford has shown that the solids precipitation occurs during processing operations from dilute Hanford liquids. Pacific Northwest National Laboratory was requested to evaluate the potential precipitated solid particle transport and flushing operational capabilities of the AP-106 through the Effluent Management Facility (EMF) low-point drain LAW feed pipeline. The evaluation results do not provide operational requirements, but rather provide a scoping basis for understanding the potential operational significance of solids precipitation in the pipeline.

The salt and aluminum phase solids most likely to precipitate from the LAW feeds during cooling, evaporation, or mixing have particle densities that are estimated to range from 1.62 to 2.78 g/mL and a spherical particle size range of 8 to 2100 µm, depending on the solid phase considered.

Application of the method to calculate the critical deposition velocity required by TFC-ENG-STD-26[1] at conservatively bounding estimates for the solids concentrations demonstrates that potentially precipitated solids may deposit on the bottom of the transfer pipe invert at the lower LAW feed pipeline flow rate of 66 gpm, but the upper LAW feed pipeline flow rate of 88 gpm will likely prevent deposition. The system pressure limit for the LAW feed pipeline from AP-106 through the EMF low-point drain of 400 psig likely exceeds any pressure loss at a calculated critical deposition velocity even for the most adverse potential precipitated solid.

However, should solids settle as a result of no-flow conditions, the flow capabilities of the LAW feed pipeline from AP-106 through the EMF low-point drain are shown, based on the available literature, to be potentially inadequate for effective flushing operations to remove solids, even at solids concentrations below the maximum specified (3.4 wt %) for LAW feed. Thus, stepwise solids accumulations over multiple transfers may be an issue, and eventual line plugging may occur. Further inadequacies may potentially be realized should the cohesive nature of certain potential precipitates such as $Na_3PO_4 \cdot 0.25NaOH \cdot 12H_2O$ and gibbsite be accounted-for.

As stated in TFC-ENG-STD-26, “[t]here is currently no accepted method to predict the transfer velocity required to re-suspend particles from a sediment bed in a waste transfer line.” This investigation asserts that, for effective flushing with respect to rate and the amount of flush liquid required to remove solids, not only must the flushing operation be conducted at a velocity that suspends single particles, the flush velocity must also be sufficient to maintain suspension as the particle concentration in the flow increases as the flow moves downstream. However, in contrast to the critical deposition velocity, which can be related to the inflow stream and can thus be predicted as a single value for a specific process stream, an effective flushing velocity must not only account for sediment erosion rate and exceed the corresponding critical velocity for the same entering fluid at a given particle concentration, it must also account for transient solids concentrations as solids are mobilized and transported downstream along the pipe.

[1] TFC-ENG-STD-26. 2019. *Waste Transfer, Dilution, and Flushing Requirements*. Rev. C-7, Washington River Protection Solutions, LLC, Richland, Washington.

Based on the scoping analyses, the following recommendations are made:

- Limited prototypic laboratory pipeline simulant testing should be conducted to confirm the scoping calculations and to substantiate the technical basis for the LAW feed flushing operations to remove solids. Confirmation of the scoping calculations must be the initial testing objective, which thereby informs, not resolves, the referenced flushing velocity basis gap in TFC-ENG-STD-26.
- Upon verification of the scoping calculation results via the limited prototypic laboratory testing, effective flushing operations should be developed or alternate feed or flushing methods should be used that mitigate the potential for accumulation of precipitated solids in the LAW feed pipeline from AP-106 through the EMF low-point drain.

# Acknowledgments

The authors thank CW Enderlin and HA Colburn for their thorough reviews, WC Dey for his QA review and support, and MS Wilburn for his technical editing.

# Acronyms and Abbreviations

| | |
|---|---|
| DFLAW | Direct Feed Low-Activity Waste |
| EMF | Effluent Management Facility |
| ICD | interface control document |
| ILST | Interim Low-Activity Waste Storage Tank |
| LAW | low-activity waste |
| PNNL | Pacific Northwest National Laboratory |
| QA | quality assurance |
| R&D | research and development |
| ROT | rule of thumb |
| RPP | River Protection Project |
| TSCR | Tank Side Cesium Removal |
| WRPS | Washington River Protection Solutions |
| WTP | Hanford Waste Treatment and Immobilization Plant |
| WWFTP | WRPS Waste Form Testing Program |

# Contents



# Figures

## Tables

# 1.0 Introduction

Pacific Northwest National Laboratory (PNNL) is providing baseline technical support to Washington River Protection Solutions (WRPS) for the Mission Integration and Waste Feed Delivery Flowsheet Integration team. Waste transfer pipeline flushing is necessary to maintain pipeline performance, but added flush fluid increases the nuclear waste inventory. During the Direct Feed Low-Activity Waste (DFLAW) mission, waste transfer lines from the Interim Low-Activity Waste Storage Tank (ILST) (i.e., 241-AP-106; hereafter AP-106) to the Hanford Waste Treatment and Immobilization Plant (WTP) Low-Activity Waste (LAW) Facility must have the capability of being flushed to prevent accumulation of solids and to mitigate corrosion concerns (Wagnon 2018).

Nguyen et al. (2016) noted that a sound technical approach to transfer-line flushing is necessary, and summarized long-term objectives to develop that technical basis to include the following:

- Establish consistent methodology for determining flush functions and objectives and defining flush requirements and parameters for the River Protection Project (RPP) mission.
- Improve Hanford flush procedures and requirements to eliminate any ambiguity and uncertainty associated with flushing operations.
- Develop benchmarked predictive tool(s) for determining and assessing flush velocities based on waste stream conditions.
- Implement a robust flush volume accounting spreadsheet tool and optimize flush strategies to improve flush efficiency and reduce volumes of flush fluid required to complete the RPP mission.
- Optimize Hanford flush operations to improve flush effectiveness and efficiency.

Specific to the second objective of Nguyen et al. (2016), this report builds on prior work from the *2019 Flushing Evaluation for the 241-AP-106 to EMF Transfer Pipeline for DFLAW*,[1] which identified potential precipitated solids from the LAW feed and examined the implications thereof for flushing based on the process stream description, corrosion, and flammable gas. For the current work, the operational capabilities and specifications for addressing potential precipitated solids of the LAW feed pipeline from AP-106 through the EMF low-point drain are compared to the TFC-ENG-STD-26 (2019) requirement for the critical deposition velocity, and to scoping estimates for the flushing velocity to remove solids and resultant pipeline pressure losses. The presented results do not provide operational requirements, but rather provide a scoping technical basis for understanding the potential operational significance of solids precipitation in the pipeline.

The identification and selection of the most probable precipitated solids for LAW feed process streams and of bounding feed and flush liquid properties are described in Section 3.0, and representative solid particle characteristics, and potential ranges of bounding bulk solid concentrations, are provided. These inputs are exercised in Section 4.0 using the TFC-ENG-STD-26 (2019) specified method to obtain critical deposition velocity, and flushing velocity estimates are made via the literature and compared to the operational capabilities specified for the LAW feed pipeline from AP-106 through the EMF low-point drain. Recommendations are provided in Section 5.0.

[1] Wells BE, LA Mahoney, EJ Berglin, CW Enderlin, RM Asmussen, and MS Fountain. 2019. *Flushing Evaluation for the 241-AP-106 to EMF Transfer Pipeline for DFLAW*, attachment to LTR-OSIF-008, Pacific Northwest National Laboratory, Richland, Washington. This is not a publicly available document.

# 2.0 Quality Assurance

This work was conducted with funding from WRPS under PNNL project 75561, contract 36437-287, with the title “One System Integrated Flowsheet.”

All research and development (R&D) work at PNNL is performed in accordance with PNNL’s Laboratory-level Quality Management Program, which is based on a graded application of NQA-1-2000, *Quality Assurance Requirements for Nuclear Facility Applications* (ASME 2000), to R&D activities. To ensure that all client quality assurance (QA) expectations were addressed, the QA controls of the WRPS Waste Form Testing Program (WWFTP) QA program were also implemented for this work. The WWFTP QA program implements the requirements of NQA-1-2008, *Quality Assurance Requirements for Nuclear Facility Applications* (ASME 2008), and NQA-1a-2009, *Addenda to ASME NQA-1-2008* (ASME 2009), and consists of the WWFTP Quality Assurance Plan (QA-WWFTP-001) and associated procedures that provide detailed instructions for implementing NQA-1 requirements for R&D work.

The work described in this report was assigned the technology level “Applied Research” and was planned, performed, documented, and reported in accordance with procedure QA-NSLW-1102, *Scientific Investigation for Applied Research*. All staff members contributing to the work received appropriate technical and QA training prior to performing quality-affecting work.

# 3.0 Potential Precipitated Solids and Process Liquid Properties

Concentrations and properties (size and density) of the potential precipitated solids from liquids in the LAW feed pipeline from AP-106 through the EMF low-point drain are described. The discussion of potential solids in this section depends on, and extends, the discussion in the 2019 DFLAW flushing evaluation.[1] The concentrations used here are upper bounds.

## 3.1 Liquids and Precipitated Solids Compositions

As previously summarized in the 2019 DFLAW flushing evaluation,[1]two types of fluids will be present in the LAW feed pipeline from AP-106 through the EMF low-point drain, based on the intended use and the existing flush supply systems. These are (1) low-cesium waste liquids treated by the Tank Side Cesium Removal (TSCR) system and stored in the ILST (i.e., AP-106), and (2) a stream that is the combination of EMF process condensate (overheads) and caustic scrubber solution (i.e., from WTP Vessel DEP-VSL-00005A/B). As presented in the 2019 DFLAW flushing evaluation[1] and discussed at more length in earlier work,[2] the salt solids that are most likely to precipitate from the low-cesium waste liquids treated by TSCR and stored in the ILST during cooling, evaporation, or mixing are NaF (sodium fluoride), $Na_7F(PO_4)_2 \cdot 19H_2O$ (natrophosphate, or sodium fluoride phosphate), $Na_3PO_4 \cdot 0.25NaOH \cdot 12H_2O$ (sodium phosphate dodecahydrate), $Na_3FSO_4$ (kogarkoite, or sodium fluoride sulfate), $Na_2CO_3 \cdot H_2O$ (thermonatrite), $Na_2C_2O_4$ (sodium oxalate), or $NaNO_3$ (sodium nitrate).

The predicted molal compositions of the liquid coming from AP-106 and the EMF condensate/scrubber liquid were obtained from model runs,[3] and were presented in the 2019 DFLAW flushing evaluation in the form of the average composition for each month in the 2021 to 2033 planned duration of the DFLAW mission. The molal composition ranges predicted for the AP-106 liquid streams can be seen in Table 1 and include only the constituents that are potential sources of the dominant types of precipitates. Since these are monthly averages that contain multiple batches, individual batches might have higher maxima and lower minima that were smoothed out by averaging. However, the time trends of the monthly averages do not show rapid changes. In molarity units, the sodium concentration range is 5.5 to 6.1 M Na.

[1] Wells BE, LA Mahoney, EJ Berglin, CW Enderlin, RM Asmussen, and MS Fountain. 2019. *Flushing Evaluation for the 241-AP-106 to EMF Transfer Pipeline for DFLAW*, attachment to LTR-OSIF-008, Pacific Northwest National Laboratory, Richland, Washington.

[2] Reynolds JG. 2019. *Bounding Salt Solubility Model for Use in WTP Waste Acceptance Criteria in the DFLAW Process*. Draft RPP-RPT-61405, Rev. 0, Washington River Protection Solutions, LLC, Richland, Washington.

[3] The predictions came from preliminary results of the March 2019 reference integrated flowsheet run (Cree et al. 2019). Source 1: "LCP Feed crosstabs Case 6858.xlsx," was received in an email to M Fountain (PNNL) from LH Cree (WRPS), "RE: Various stream compositions for DFLAW flushing assessment," 5/7/2019. Source 2: "WTP to LERF crosstabs Case 6858.xlsx," was received in an email to LA Mahoney (PNNL) from LH Cree (WRPS), "Waste streams recommended for use as flush water," 5/14/2019.

Table 1. Predicted composition range for AP-106 supernatant from monthly averages over mission.

| Chemical Species | Maximum Concentration (m) | Median Concentration (m) | Minimum Concentration (m) |
|---|---|---|---|
| $Al(OH)_4^-$ | 0.193 | 0.123 | 0.0656 |
| $C_2O_4^{-2}$ | 0.0111 | 0.00936 | 0.00571 |
| $F^-$ | 0.0543 | 0.0245 | 0.0105 |
| $Cl^-$ | 0.103 | 0.0885 | 0.0517 |
| $Na^+$ | 6.84 | 6.22 | 6.15 |
| $NO_2^-$ | 1.31 | 1.20 | 0.977 |
| $NO_3^-$ | 3.23 | 2.12 | 1.67 |
| $OH^-$ | 2.49 | 1.59 | 0.887 |
| $PO_4^{-3}$ | 0.0571 | 0.0262 | 0.0189 |
| $SO_4^{-2}$ | 0.0676 | 0.0526 | 0.0196 |
| $CO_3^{-2}$ | 0.674 | 0.522 | 0.211 |

Of the listed salt solids, it has been demonstrated[1] that $NaNO_3$ will not precipitate below a total sodium molality of 8.7 even when the only other anion in solution is hydroxide, which is the co-anion (of those that are dominant in waste) that has the greatest effect in reducing $NaNO_3$ solubility (Reynolds 2018). It has also been demonstrated that when the total sodium molarity is 5 to 6, $Na_2CO_3 \cdot H_2O$ should be soluble in NaOH solution between 0 ºC and 100 ºC so long as the sodium carbonate molality is less than 0.6 m (Cree et al. 2017). That assessment was based on solutions where the only co-anion was hydroxide, which means that the presence of nitrate and nitrite would lead to higher $Na_2CO_3 \cdot H_2O$ solubility and less precipitation. A later study (Reynolds 2017) discussed carbonate solutions containing a different co-anion (nitrate) and concluded that $Na_2CO_3 \cdot H_2O$ would not precipitate at for sodium molality less than about 8.4. Thus, based on the concentrations in Table 1, $NaNO_3$ and $Na_2CO_3 \cdot H_2O$ are not expected to precipitate.

The remaining salt solids of concern in the transfer line are $Na_7F(PO_4)_2 \cdot 19H_2O$, $Na_3PO_4 \cdot 0.25NaOH \cdot 12H_2O$, kogarkoite, NaF, and $Na_2C_2O_4$. Aluminum hydroxide ($\gamma$-$Al(OH)_3$) is also a potential precipitate from dissolved aluminum at the hydroxide concentrations present in the streams in Table 1 (Reynolds and Reynolds 2010). The salts are likelier to precipitate in undiluted AP-106 supernatant because of temperature decreases in the pipeline or evaporation during periods when there is no flow, while aluminum hydroxide could precipitate because of cooling, dilution of supernatant hydroxide with flushing liquid (EMF condensate/scrubber liquid), or both.

The salts $Na_3PO_4 \cdot 0.25NaOH \cdot 12H_2O$ and $Na_7F(PO_4)_2 \cdot 19H_2O$ have been demonstrated to precipitate at liquid concentrations similar to those in Table 1 at temperatures that could occur in the transfer line. In a set of tests (Mahoney and Russell 2006) that employed 241-S-109 simulants, precipitation of 5 vol% solids or more was observed within 3 days when temperatures of 40 and 50 °F (4 to 10 °C) were applied to a 6 M Na simulant containing aluminate, nitrite, nitrate (the dominant anion), hydroxide, phosphate, sulfate, carbonate, and other anions, but no oxalate or fluoride. Needle-shaped solids consistent with $Na_3PO_4 \cdot 0.25NaOH \cdot 12H_2O$ and unidentified smaller white crystals were observed. In an early version of the simulant that included fluoride, 0.5 to 1 vol% of $Na_7F(PO_4)_2 \cdot 19H_2O$ appeared at 70 to 75 °F (21 to 24 °C) when concentrations were respectively 6 M Na and 7 M Na. The precipitate was estimated to contain more than half the fluoride originally present in the recipe.

The plausible precipitated solids, $Na_3PO_4 \cdot 0.25NaOH \cdot 12H_2O$ and aluminum hydroxide, can form gels, and $Na_7F(PO_4)_2 \cdot 19H_2O$, whose precipitation rapidly produces large particles. By comparison, kogarkoite,

[1] *Bounding Salt Solubility Model for Use in WTP Waste Acceptance Criteria in the DFLAW Process*

NaF, and $Na_2C_2O_4$ are constrained by lower concentrations in the liquid. The fluoride compounds kogarkoite and NaF are likely to be out-competed by $Na_7F(PO_4)_2 \cdot 19H_2O$, and therefore are less likely to be present.

## 3.2 Precipitated Solids Properties

The Hanford waste properties summary report (Wells et al. 2011) developed a set of primary particle densities, shape factors, and maximum primary particle spherical diameters (equivalent on a volume basis) for a wide range of solid phases observed in Hanford waste. The data for the solids of interest in the transfer line have been extracted into Table 2.[1]

The large in-tank primary particle sizes given in Table 2 were observed in waste particles that had been growing with little disturbance for years in the tanks. However, there is a maximum 14-day limit on the delay between a transfer and a flush (or subsequent transfer) (TFC-ENG-STD-26 2019). If line flushing is adequate to remove precipitate after every use of the transfer line, the precipitate in the line can be present as smaller primary particles than the in-tank maximum sizes because the time limit truncates the growth The probable time-limited maximum primary particle sizes of the dominant transfer-line solid phases are estimated below, for the major solids, and are also summarized in Table 2. No estimates were made for $Na_2C_2O_4$, $Na_3FSO_4$, or NaF because they were estimated to be present at trivial or zero concentrations in the upper-bound precipitation estimates that are presented in Section 3.4.

[1] The maximum primary particle spherical diameters are selected as representative for this scoping evaluation. In actuality, as evidenced by the "maximum" notation, the primary particles are distributed in size, and the waste usually contains mixtures of primary particles and their composite agglomerates. While the selection of the maximum particle size can be bounding, it is also noted in Wells et al. (2011) that the primary particles can form agglomerates of any size within the measured waste's size range, regardless of the size of the primary particles. Given that the measured waste's size range (e.g., of a given tank waste) is typically larger than the maximum primary particle sizes, the use of these maximum sizes may, in fact, not be bounding. Of course, as agglomerates are formed, the effective particle density is reduced via inter-particle porosity. However, with respect to particle density, Lee et al. (2012) note, "There is no conclusive evidence that representing the particle density of Hanford waste particles by assuming that all particles have a density equal to the UDS [undissolved solid] compound crystal density regardless of the measured particle size … over-represents the settling characteristics of particles suspended by jet mixer pump operation" (bracketed text added). Thus, the use of the primary particle size and density for the potential precipitated solids is deemed appropriate.

Table 2. Primary particle properties for potential precipitated solids.

| Solid Phase | Primary Particle Density (g/mL) | Shape Factor | In-Tank Maximum Spherical Primary Particle Diameter (μm) | 14-Day Maximum Spherical Primary Particle Diameter (μm) |
|---|---|---|---|---|
| $Al(OH)_3$ (gibbsite, aluminum hydroxide) | 2.42 | n/a | 200 | 50 |
| $Na_2C_2O_4$ (sodium oxalate) | 2.34 | 0.4 | 8 | Not estimated |
| $Na_3FSO_4$ (kogarkoite, sodium fluoride sulfate) | 2.65 | 0.8 | 176 | Not estimated |
| $Na_3PO_4 \cdot 0.25NaOH \cdot 12H_2O$ (sodium phosphate dodecahydrate) | 1.62 | 0.4 | 440 | 250 |
| NaF (sodium fluoride) | 2.78 | n/a | 12 | Not estimated |
| $Na_7F(PO_4)_2 \cdot 19H_2O$ (natrophosphate, sodium fluoride phosphate) | 1.75 | n/a | 2100 | 500 |

Sodium phosphate dodecahydrate ($Na_3PO_4 \cdot 0.25NaOH \cdot 12H_2O$) forms needle-like primary crystals with high aspect ratios that settle into a gel.[1] Herting et al. (2002) refer to an aspect ratio greater than 10 for this solid phase; some of the Hanford waste images in that reference suggest ratios of 15, perhaps greater. The high aspect ratio is the reason for the low shape factor. A study of $Na_3PO_4 \cdot 0.25NaOH \cdot 12H_2O$ and $Na_7F(PO_4)_2 \cdot 19H_2O$ precipitation in simulants (Reynolds and Herting 2016) demonstrated that $Na_3PO_4 \cdot 0.25NaOH \cdot 12H_2O$ precipitation could produce needles up to 1000 μm long within 4 days. At an aspect ratio of 10, these needles would have a volume-based spherical diameter of about 250 μm; at an aspect ratio of 15, the spherical-equivalent diameter would have been about 190 μm. Smaller needles were seen on the first day of the experiment – up to 400 μm long, with spherical diameters in the range of 80 to 100 μm. For the high-fluoride (0.1 M F) and high-phosphate (0.2 M $PO_4$) simulants used in the experiment, the initial precipitate of $Na_3PO_4 \cdot 0.25NaOH \cdot 12H_2O$ recrystallized to $Na_7F(PO_4)_2 \cdot 19H_2O$ between 4 and 17 days. As a result, $Na_3PO_4 \cdot 0.25NaOH \cdot 12H_2O$ crystals did not continue to grow past the 1000-μm size. If less fluoride were present, the growth of $Na_3PO_4 \cdot 0.25NaOH \cdot 12H_2O$ crystal could continue.

Natrophosphate ($Na_7F(PO_4)_2 \cdot 19H_2O$) forms compact octahedral and cuboctahedral primary crystals (Herting et al. 2002). Their bulky, near-spherical shape gives them a high shape factor. In the simulant experiment already cited, $Na_7F(PO_4)_2 \cdot 19H_2O$ octahedra of about 100 μm in size had precipitated at 4 days, while at 17 days the $Na_7F(PO_4)_2 \cdot 19H_2O$ precipitate was composed mostly of particles in the 50- to 200-μm size range, with a few at 500 μm or larger. A spherical diameter of 500 μm is a reasonable maximum for $Na_7F(PO_4)_2 \cdot 19H_2O$ particles under time-limited conditions.

There are no experimental data for gibbsite to support a direct estimate of time-limited sizes for gibbsite primary particles. However, gibbsite is generally expected to precipitate more slowly than do the salts, as discussed in the 2019 DFLAW flushing evaluation.[2] The slower precipitation rate for gibbsite implies a

[1] Sodium oxalate ($Na_2C_2O_4$) also characteristically produces needles, but both the aspect ratio and the particle size are smaller than for $Na_3PO_4 \cdot 0.25NaOH \cdot 12H_2O$. Wells et al. (2011) estimated the same shape factor for $Na_2C_2O_4$ as for $Na_3PO_4 \cdot 0.25NaOH \cdot 12H_2O$. Recent work (Bolling et al. 2017) discovered that under some tank conditions, as in tank 241-AP-107, $Na_3FSO_4$ can appear as needles, and not just in the previously observed isotropic hexagons. When found in needle habit, the shape factor of $Na_3FSO_4$ would probably be less than 0.5, as for $Na_3PO_4 \cdot 0.25NaOH \cdot 12H_2O$ and $Na_2C_2O_4$.

[2] *Flushing Evaluation for the 241-AP-106 to EMF Transfer Pipeline for DFLAW*.

reduced particle growth rate compared to that for salts. As a result, the time-limited primary gibbsite particle sizes would not approach the in-tank sizes as closely as the salt sizes would. Therefore, the ratio of time-limited maximum size to in-tank maximum size is likely to be smaller than for the salts. As estimated above, the ratio of time-limited maximum diameter to in-tank maximum diameter is about 1:4 for $Na_3PO_4 \cdot 0.25NaOH \cdot 12H_2O$ at 1 day, 1:2 for $Na_3PO_4 \cdot 0.25NaOH \cdot 12H_2O$ at 4 days, 1:20 for $Na_7F(PO_4)_2 \cdot 19H_2O$ at 4 days, and 1:4 for $Na_7F(PO_4)_2 \cdot 19H_2O$ at 17 days. Applying a ratio of 1:4, and assuming an in-tank maximum primary particle spherical diameter of 200 µm, gives a time-limited maximum primary particle spherical diameter of 50 µm for gibbsite at 14 days. This is considered to be an upper bound.

## 3.3 Process Liquid Properties

Based on the 2019 DFLAW flushing evaluation[1]evaluation[1], the maximum expected liquid density in the transfer pipeline is 1.285 kg/L, for the AP-106 supernatant stream with the highest density. The minimum liquid density is that of the EMF condensate/scrubber liquid, 1.00 kg/L.[2] Liquids with maximum and minimum density are both pertinent to aluminum hydroxide precipitation, but the minimum-density liquid would not be present at the same time as salt precipitate (because the salt would dissolve).

Tank waste liquid viscosities can be approximately correlated with the liquid densities, using the low-density form of Equation (5-3) of Meacham et al. (2012):

$$\mu = exp\left(-18.29(\rho - 1) + \frac{7103.79(\rho - 1) + 54.36}{T}\right) \quad (1)$$

where

$\mu$ = liquid viscosity, cP
$\rho$ = liquid density, g/mL
$T$ = absolute temperature, K

The minimum-density liquid in the transfer line is the condensate/scrubber liquid. Its viscosity at 20 °C is 1.2 cP. For comparison, the standard value for the viscosity of water at that temperature is 1.0 cP (CRC 1976).

The maximum-density AP-106 supernatant is predicted to have a viscosity of 6.5 cP at 20 °C. Table B-1 of Meacham et al. (2012) indicates that waste liquids whose densities are 1.3 g/mL or less at 20 to 30 °C typically have viscosities that are less than or about equal to the predicted values. Out of 11 measurements, one was an exception – AN-104 liquid with a density of 1.3 g/mL had a measured viscosity of 17.5 cP and a predicted viscosity of 6.3 cP at 25 °C. In general, though, the viscosity of AP-106 supernatant would be expected to be less than about 7 cP.

The viscosity model presented in Meacham et al. (2012) is recognized as tending to overpredict viscosity. A more complex model that uses composition data to evaluate terms for ion-ion interactions has been shown to provide more accurate viscosity estimates (Daniel et al. 2018), but the higher viscosity given by Eq. (1), as used above, serves to provide a probable upper bound for liquid viscosity for the present application.

[1] *Flushing Evaluation for the 241-AP-106 to EMF Transfer Pipeline for DFLAW*.
[2] Wagnon (2018) recommended flushing per TFC-ENG-STD-26 (2019) and using EMF process condensate (which will be combined with caustic scrubber solution) as the best available path forward.

## 3.4 Precipitated Solids Concentrations

The absolute upper-bound estimates of precipitation in the 2019 DFLAW flushing evaluation[1] followed an approach used in earlier work.[2] A completely bounding assumption was made that the ionic species that potentially produce precipitate – fluoride, phosphate, oxalate, and aluminate – had zero solubility and would drop completely out of solution to form precipitate. In actuality, some amounts of each species would remain behind in solution, according to the relative solubilities of the different solid phases at whatever temperatures and solution compositions were present. This approach is unphysical but produces an ultimate upper bound for screening purposes.

Note, though, that the result of this approach is an upper bound only for each month's total transfer of waste. If solids deposit and are not completely flushed from the pipe system, accumulation could lead to higher solids concentrations in part or all of the line.

Three different types of bounding assumptions were tested, two covering situations where salt precipitation was of the most concern and one covering situations where dilution occurs. In Case 1, the production of large $Na_7F(PO_4)_2 \cdot 19H_2O$ particles was the design concern because of potential difficulties with resuspension. The total possible $Na_7F(PO_4)_2 \cdot 19H_2O$ precipitation was calculated, with precipitation of other fluoride and phosphate salts being limited to what was left over after $Na_7F(PO_4)_2 \cdot 19H_2O$ had dropped out. Sodium fluoride sulfate was dropped out before NaF, so the latter precipitate appeared only if there was fluoride left over after what was consumed by the available phosphate and sulfate. In Case 2, the production of $Na_3PO_4 \cdot 0.25NaOH \cdot 12H_2O$ gel was the design concern. The total possible $Na_3PO_4 \cdot 0.25NaOH \cdot 12H_2O$ precipitation was calculated, with subsequent precipitation of $Na_7F(PO_4)_2 \cdot 19H_2O$, followed by sodium fluoride sulfate, followed by NaF. Finally, in Case 3, the total possible aluminum hydroxide gel precipitation was calculated. The sodium salts present at the maximum dissolved aluminum concentration were assumed to precipitate in the Case 2 manner to maximize gel. In all three cases, the $Na_2C_2O_4$ was also assumed to completely precipitate.

The assessment of mixing of streams was also handled using a bounding approach. Every monthly-average AP-106 stream was assumed to mix with every other AP-106 or EMF condensate/scrubber liquid stream produced during the DFLAW mission for 2021 to 2033, even if they were not predicted to occur close together in time. This approach was intended to offset any underestimation of maximum batch concentrations that may have occurred because of monthly averaging. Each combination of streams was assumed to occur with a mixing fraction of 10% of one stream and 90% of the other, 20% of the first and 80% of the second, etc., so that all the different proportions that might be present were considered. For each combination of streams and each mixing fraction, the Case 1, Case 2, and Case 3 solids were calculated. This allowed the maximum solids to be found for each of the cases, over all combinations and mixing fractions. For Case 3, it was assumed that aluminum was precipitating as the result of dilution and that salts did not precipitate.

The results were as follows for three different maximum precipitation cases:

- Case 1: The maximum $Na_7F(PO_4)_2 \cdot 19H_2O$ solids concentration was 2.60 wt%, accompanied by 0.21 wt% $Na_2C_2O_4$. There was not enough phosphate left, under the assumed constraints, to provide enough $Na_3PO_4 \cdot 0.25NaOH \cdot 12H_2O$ gel to show up at the second decimal place. If both hydroxide dilution and double-salt combination were to occur, 1.19 wt% aluminum hydroxide gel would accompany the potentially large $Na_7F(PO_4)_2 \cdot 19H_2O$ particles. At the maximum liquid density of

[1] *Flushing Evaluation for the 241-AP-106 to EMF Transfer Pipeline for DFLAW.*
[2] *Bounding Salt Solubility Model for Use in WTP Waste Acceptance Criteria in the DFLAW Process*.

1.285 g/mL, the volume percent solids would be 0.64 vol% gibbsite, 0.12 vol% $Na_2C_2O_4$, and 1.94 vol% $Na_7F(PO_4)_2 \cdot 19H_2O$.

- Case 2: The maximum $Na_3PO_4 \cdot 0.25NaOH \cdot 12H_2O$ gel solids concentration was 3.22 wt%, accompanied by 0.32 wt% kogarkoite and 0.21 wt% $Na_2C_2O_4$. There was not enough fluoride or phosphate left, under the assumed constraints, to produce $Na_7F(PO_4)_2 \cdot 19H_2O$ or NaF. If hydroxide dilution also occurred, 0.91 wt% aluminum hydroxide gel would accompany the $Na_3PO_4 \cdot 0.25NaOH \cdot 12H_2O$ gel. At the maximum liquid density of 1.285 g/mL, the volume percent solids would be 0.49 vol% gibbsite, 0.12 vol% $Na_2C_2O_4$, 0.16 vol% kogarkoite, and 2.59 vol% $Na_3PO_4 \cdot 0.25NaOH \cdot 12H_2O$.
- Case 3: The maximum aluminum hydroxide gel solids concentration, assumed to be free of salt solids because of dilution, was 2.15 wt%. At the maximum liquid density of 1.285 g/mL, the corresponding volume percent solid would be 1.15 vol%, and at the minimum liquid density of 1.00 g/mL, the corresponding volume percent solid would be 0.90 vol%.

Table 3 summarizes the above concentration information.

Table 3. Case summary of potential precipitated solids concentrations.

| | Case 1 | | | Case 2 | | | Case 3 | | |
|---|---|---|---|---|---|---|---|---|---|
| Solid Phase | wt% | vol% in Max. Density Liquid | vol% in Min. Density Liquid | wt% | vol% in Max. Density Liquid | vol% in Min. Density Liquid | wt% | vol% in Max. Density Liquid | vol% in Min. Density Liquid |
| $Al(OH)_3$ (gibbsite, aluminum hydroxide) | 1.19 | 0.64 | 0.50 | 0.91 | 0.49 | 0.38 | 2.15 | 1.15 | 0.90 |
| $Na_2C_2O_4$ (sodium oxalate) | 0.21 | 0.12 | Dissolved | 0.21 | 0.12 | Dissolved | n/c | n/c | Dissolved |
| $Na_3FSO_4$ (kogarkoite, sodium fluoride sulfate) | n/c | n/c | Dissolved | 0.32 | 0.16 | Dissolved | n/c | n/c | Dissolved |
| $Na_3PO_4 \cdot 0.25NaOH \cdot 12H_2O$ (sodium phosphate dodecahydrate) | n/c | n/c | Dissolved | 3.22 | 2.59 | Dissolved | n/c | n/c | Dissolved |
| NaF (sodium fluoride) | n/c | n/c | Dissolved | n/c | n/c | Dissolved | n/c | n/c | Dissolved |
| $Na_7F(PO_4)_2 \cdot 19H_2O$ (natrophosphate, sodium fluoride phosphate) | 2.60 | 1.94 | Dissolved | n/c | n/c | Dissolved | n/c | n/c | Dissolved |
| Total | 4.00 | 2.70 | 0.50 | 4.66 | 3.36 | 0.38 | 2.15 | 1.15 | 0.90 |

"n/c": This solid is not present in the case.
"Dissolved": Salts are assumed to have been dissolved for the minimum-density liquid (effectively water).

# 4.0 Transfer and Flushing Evaluation of Precipitated Solids

The properties of the precipitated solids described in Section 3.0 are employed in evaluating potential transfer and flushing performance in the LAW feed pipeline from AP-106 through the EMF low-point drain. First, to evaluate the potential for precipitated solids to deposit in the pipeline during waste transfer, critical deposition velocities are calculated.[1] Second, in the event that deposition does occur during transport, or settling of the precipitated solids occurs in the absence of flow (i.e., between transfers or between a transfer and a flushing operation), the velocity required to resuspend the solid particles is considered (herein termed the "flush velocity").[2] The calculated velocity results are then compared to the AP-106 to WTP LAW feed pipeline operating capabilities for flow rate (velocity) and pressure.

It is emphasized that the calculations presented herein do not provide operational requirements. Instead, as discussed in Section 1.0, the calculations provide a scoping basis for the understanding of the potential operational significance of solids precipitation in the LAW feed pipeline from AP-106 through the EMF low-point drain.

## 4.1 Calculation Methodology

The calculation methodologies are presented for critical deposition velocity and flush velocity.

### 4.1.1 Critical Deposition Velocity

TFC-ENG-STD-26 (2019) requires that the critical velocity for concentrated supernatant and slurry (both terms defined therein) transfers is calculated using the methodology of Oroskar and Turian (1980), and that model will therefore be employed for this evaluation. The commonly employed form of the Oroskar and Turian critical velocity ($U_C$) model is

$$U_C = 1.85\sqrt{gd(S-1)}\phi^{0.1536}(1-\phi)^{0.3564}\left(\frac{d}{D}\right)^{-0.378}\left[\frac{D\rho\sqrt{gd(S-1)}}{\mu}\right]^{0.09}\chi^{0.30} \quad (2)$$

where

- $g$ = gravitational acceleration
- $d$ = spherical particle diameter (see Section 3.0)
- $S$ = ratio of the solid density to the liquid density (see Section 3.0)
- $\phi$ = solid volume fraction (volume of solids per total volume) (see Section 3.0)
- $D$ = pipe diameter (inside diameter of a 3-inch Schedule 40 pipe)
- $\chi$ = fraction of eddies having velocities equal to or greater than the settling velocity. $\chi$ is typically set to 0.96 (e.g., Wells et al. 2007)
- $\rho$ = carrier liquid density (see Section 3.0)
- $\mu$ = carrier liquid viscosity (see Section 3.0)

[1] TFC-ENG-STD-26 (2019) defines the critical deposition velocity as the velocity needed to ensure that solids are not deposited in the transfer piping.

[2] TFC-ENG-STD-26 (2019) defines the flush velocity as the transfer velocity required to resuspend particles from a sediment bed in a waste transfer line.

TFC-ENG-STD-26 (2019) requires a factor of 1.3 to be applied to the calculated critical velocity as a design margin. The Oroskar-Turian model does not take into account the effects of polydisperse solids because a single value is entered (each) for particle size, particle density, and solid concentration. Hanford waste in general is significantly polydisperse (e.g., Wells et al. 2011) and the precipitated solids described in Section 3.0 are clearly non-uniform. Turian et al. (1987) compared the model predictions to a collection of 864 data points for critical velocity. The data points included solid densities of 1.15 to 7.475 g/mL, fluid densities of 0.77 to 1.35 g/mL, fluid viscosities of 0.77 to 38 cP, particle sizes of 20 to 19,000 µm, and solids concentrations as low as 0.5 vol% and as high as 50 vol% [note that a maximum $U_C$ is achieved via the Oroskar and Turian model at $\phi$ between 0.25 and 0.3, (Turian et al. 1987)]. Thus, the individual solids and liquid properties described in Section 3.0 are generally represented.

### 4.1.2 Flush Velocity

Nguyen et al. (2016) noted that most facility requirements safeguard against transfer line plugs via management of minimum transport velocity based on determination of the critical velocity, and that flushing is intended to prevent plugging resulting from settled and accumulated solids. It is well established in the literature that, for a given suspending fluid, the flow velocity required to suspend a particle (resuspension velocity) is greater than the velocity required to keep that particle in suspension (transportation or deposition velocity), e.g., Figure 1 (Schwuger 1996, from Hjulström 1935). Likewise, from Nguyen et al. (2016), the flush velocity must exceed the corresponding critical velocity for the same entering fluid because only flushing velocities that exceed the critical velocity can resuspend and mobilize particles. Therefore, a question of interest is, for a given solid/fluid condition, by how much does the flush velocity need to exceed the critical velocity?

From Figure 1 for open channel flow, the extent to which the flow velocity for particle resuspension exceeds the transportation/deposition velocity for a corresponding particle size varies significantly (see also Bagnold 1941; Mantz 1977 discusses the increasing resuspension velocity below the minima with decreasing particle size). From the Figure 1 example nominally above the minima for resuspension velocity (or just above 100 µm, or 0.1 mm), the resuspension velocity is shown to range from approximately 1.5 to more than 10 times the deposition velocity.

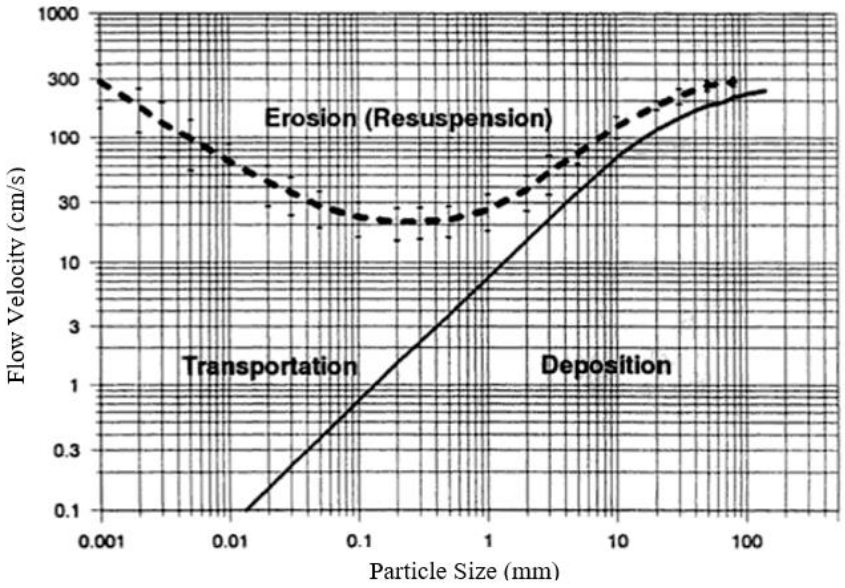


Figure 1. Particle transportation (critical deposition) and resuspension (flush) velocities as a function of particle size in water (from Schwuger 1996). Monodispersed particles at a constant particle density of 2.65 g/mL.

In their review of flushing practices in municipal systems, Nguyen et al. (2016) summarized flushing velocities relative to normal operational velocities in the range of 1.3 to 1.8. Zenz (1964) investigated the minimum velocities required to convey single particles [of varied size (~10 to 6350 µm), density, and shape] in horizontally flowing air and water in 1.25-inch and 2.5-inch pipes. He correlated the experimentally determined velocities with the Reynolds number in terms of the conventional drag coefficient and noted agreement with measurements of sand movements in the open desert (i.e., Bagnold 1941). Although Zenz (1964) did not extensively investigate the minimum velocity required to pick up a particle from a layer of particles and transport it through the pipe, it was reported that the data obtained showed it to give velocities 2 to 2.5 times higher than the minimum velocity required to transport a particle without deposition and without obviously rolling or bouncing (i.e., the particle remained in suspension).

Poloski et al. (2009) performed complex simulant testing of Hanford waste simulants for the deposition velocities of non-Newtonian slurries in pipes and concluded that, for the conditions tested, “Flushing at 10 ft/s or more should be sufficient to remove the sediment beds. However, re-suspension of particles from a stationary bed involves different mechanics from deposition.” and “The design-basis value for the minimum flush velocity to remove a stationary bed should be supported by further testing.” For their tests with 150-µm glass beads in non-Newtonian slurries with Casson yield stress varying from 0.3 to 31 Pa, the deposition velocity ranged from 2 to 5 ft/s. Testing with a high-level waste simulant with Casson yield stress varying from 3.1 to 27 Pa resulted in deposition velocities ranging from 2.5 to 5 ft/s. “Loose” comparison (i.e., flushes at 10 ft/s were sufficient to remove the sediment beds, but case-by-case flushing velocities were not reported) of the 10 ft/s flush velocity to the critical deposition velocity test results provides ratios of 2 to 4.

Nguyen et al. (2016) discussed in detail that, although the current Hanford Site projected WTP operations use the Oroskar and Turian (1980) model as a basis for determining flush velocities for solids removal, the physical mechanisms for resuspending particles in a pipeline differ from those that control initial particle deposition. As a result, Nguyen et al. (2016) recommend that the minimum flush velocity predicted by the projected WTP operations use of the Oroskar and Turian (1980) model should be

implemented with caution and its use be re-evaluated. Note that the technical arguments and cautions do not alter the requirement that the flush velocity must exceed the corresponding critical velocity for the same entering fluid. Rather, they call into question the methodology employed to determine the flush velocity required for the successful resuspension and removal of particles from a sediment bed in a waste transfer line.

A flush velocity model is considered herein to investigate the amount by which the flush velocity needs to exceed the critical velocity, depending on particle properties. These flushing velocity calculations provide a scoping basis for the understanding of the potential operational significance of solids precipitated in the AP-106 to WTP LAW feed pipeline. The effect of the varied precipitated solids properties (Section 3.2) must be accounted-for given the noted variation in the flush velocity-to-critical velocity ratio with particle properties (e.g., Figure 1). To calculate flush velocity, TFC-ENG-STD-26 (2019) states, "There is currently no accepted method to predict the transfer velocity required to re-suspend particles from a sediment bed in a waste transfer line." A minimum flush velocity model is presented in Nguyen et al. (2016). However, as advised therein, benchmarking of that pipeline-flushing model against experimental data specific to pipeline flushing data is recommended to complete its validation for implementing as a field operations tool. Thus, an initial cursory selection of a flush velocity model is made from the literature.

Rabinovich and Kalman (2011) provide a literature review that compares and analyzes previously published investigations on various threshold velocities of the two-phase (fluid-solids) flow in horizontal systems, including incipient motion, pickup from a layer of particles, pickup from heap-shaped particles deposits, boundary saltation, and minimum pressure velocities. The former three threshold velocities can be related to flush velocity, while the latter two address deposition velocity. From the 16 reviewed correlations for incipient motion/pickup velocity, the model of Rabinovich and Kalman (2007) is most germane to flushing the AP-106 to WTP LAW feed pipeline as the model's dataset includes the data for hydraulic flow in horizontal pipes (from Ramadan et al. 2003), albeit in a very limited amount.

Rabinovich and Kalman (2007) present experimental results on pickup velocity measurements for a variety of particulate solids in gases and in liquids. An empirical relationship for the pickup velocity of a particle from a layer of particles in liquids (134 data points) in the form of modified Reynolds and Archimedes numbers is provided, Figure 2. Also included in Figure 2 are pickup velocity data in gases. Rabinovich and Kalman (2007) state: "As expected, the pickup velocity results of particles by liquids overlap the results in gas–particle systems at Zone I and continue the same slope also for smaller Archimedes numbers at Zones II and III. Therefore, the pickup results can be predicted by a simple empirical relationship at an error of ± 30% over the tested range".[1] The empirical model is given by

[1] From Rabinovich and Kalman (2007), Zone I ($Ar > 16.5$) represents negligible cohesion forces, Zone II ($0.45 \leq Ar \leq 16.5$) represents considerable cohesion forces that increase the required pickup velocity of individual particles, and Zone III ($Ar < 0.45$) represents significant cohesion forces that cause pickup of agglomerates. This result is unique in comparison with other literature (e.g., Vanoni 1975; Julien 1998; Mantz 1977) but is not accounted-for in the current work. To restate, the effect of particle cohesion, or absence of effect, is not addressed in this current work. Further, the potential precipitated particles that have size and density that correspond to a modified Archimedes number of less than 0.01 (see Rabinovich and Kalman 2011) are not evaluated via Eq. (2).

$$Re_p^* = 5Ar^{*\frac{3}{7}} \quad (3)$$

where

$Re_p^*$ = modified Reynolds number, $Re_p^* = \frac{\rho U_{pu} d}{\mu\left(1.4-0.8e^{-\frac{\frac{D}{D_{50}}}{1.5}}\right)}$

$U_{pu}$ = pickup velocity

$D_{50}$ = reference pipe internal diameter of 50 mm

$Ar^*$ = modified Archimedes number, $Ar^* = \frac{(S-1)gd^3}{\upsilon^2}(0.03e^{3.5\omega})$

$\nu$ = liquid kinematic viscosity $\left(\frac{\mu}{\rho}\right)$

$\omega$ = particle sphericity (set to 1, see Section 3.0)

The modified Reynolds number takes into account pipe diameter, and the modified Archimedes number addresses particle shape. The data of Ramadan et al. (2003) for tests in horizontal pipes (solid circles in Figure 2; difficult to discern), are shown to lie within the data set.

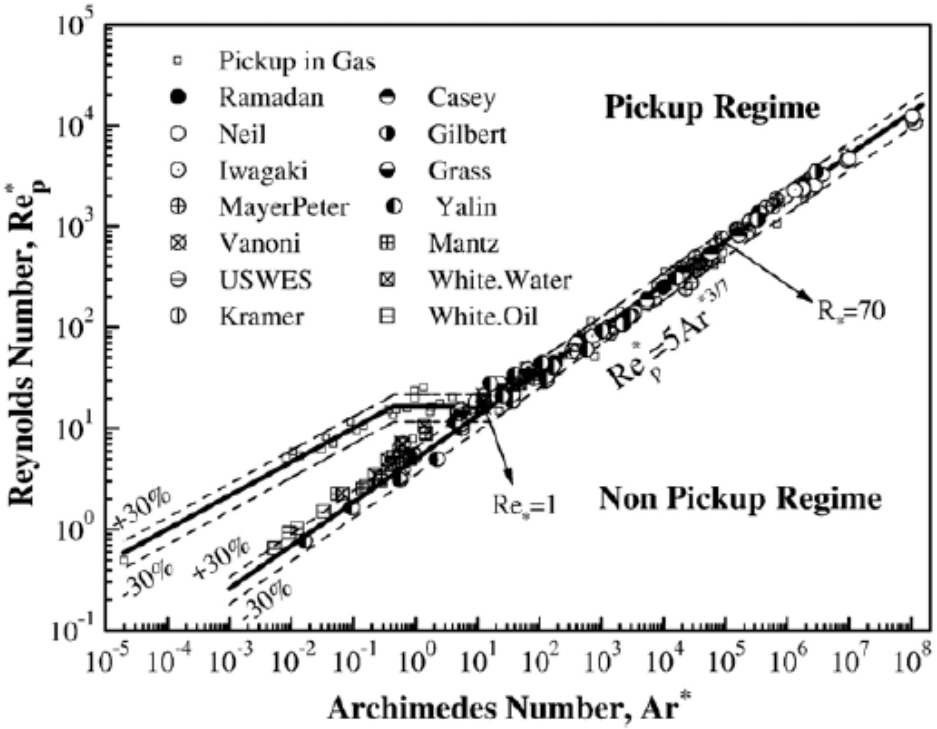


Figure 2. Pickup velocity of particles in gases and in liquids (from Rabinovich and Kalman 2007).

Note that the Rabinovich and Kalman (2007) model for the pickup velocity of particles from a sediment would likely not provide an efficient flushing velocity as will be described. Wells et al. (2009) provide a qualitative graphical representation of the erosion rate of a sediment material as a function of applied

stress for a single material, provided herein as Figure 3. The plot is labeled with the regions of stable bed, surface erosion, mass erosion, and complete failure associated with increasing rates of erosion. The onset of erosion, i.e., the pickup of individual particles from a sediment, provides a minimum erosion rate, and therefore a minimum initial flushing velocity.

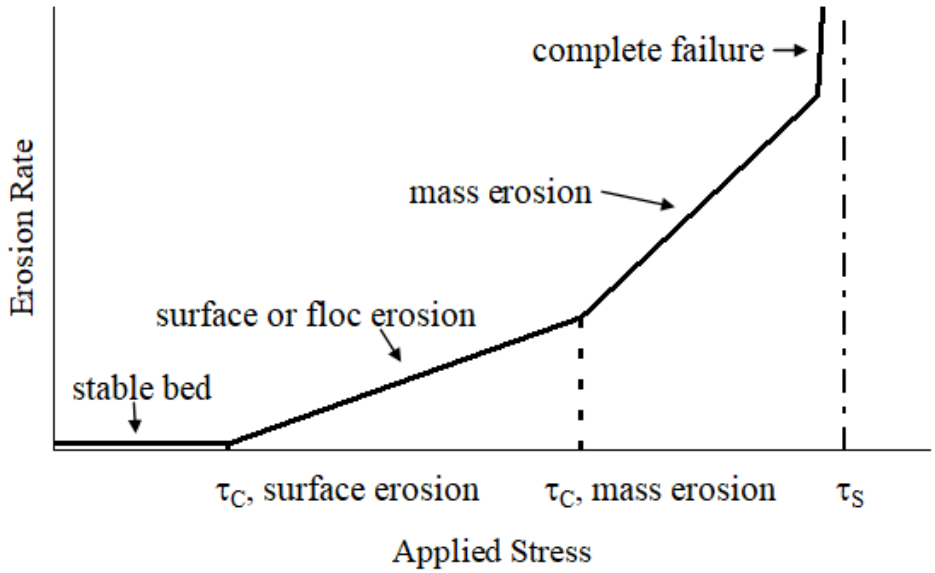


Figure 3. Graphical qualitative representation of the erosion rate as a function of applied stress for a single material (from Wells et al. 2009). $\tau_C$ indicates the critical applied stresses for the different erosion regions, and complete failure (i.e., complete resuspension) is shown to occur at an applied stress approaching the sediment material's yield stress in shear $\tau_S$.

For illustrative purposes, Figure 4 provides a simplistic comparison of the calculated critical velocity [Oroskar and Turian 1980 model, Eq. (2)] representing the hydraulic pipeline test conditions of the Ramadan et al. (2003) tests included in Rabinovich and Kalman (2007), to the measured pickup velocities. The critical velocities are calculated using the minimum concentration of Turian et al. (1987), 0.5 vol%. This simple example comparison, providing results that suggest that the calculated critical velocities exceed the measured pickup velocities, aptly illustrates a difficulty of relating critical velocity model results to single particle pickup velocities; particle concentration affects the results, as expected [e.g., see Figure 3 and Eq. (2)].

As described in detail in Nguyen et al. (2016), the deposition and resuspension of solids in a pipeline is a complex process, and transients in flow characteristics and process piping component configurations can exacerbate the issues presented by solids concentrations. Here, a simple example is described. Consider an initial condition for a flushing operation wherein a pipeline flow is stopped, no gravity drain occurs, precipitated solids are present at concentrations as described in Section 3.2, and a sediment at the bottom of the pipe invert is formed by particles settling after the cessation of flow. If a flushing operation is conducted at a velocity that suspends single particles, there is a potential that at some distance downstream, as particles are picked up at each incremental distance, the suspended solids concentration in the flow will render the flush velocity insufficient to maintain suspension, and redeposition can occur (e.g., Figure 4). Thus, not only must a flush velocity be set to effectively (see Figure 3) resuspend settled solid particles, the flow must also be sufficient to maintain those particles in suspension as the concentration of particles in the flow increases as the flow continues downstream. Of course, there is the

potential for many competing effects; e.g., solids loading in the flush liquid increases the apparent liquid density, thereby decreasing the pickup and critical velocities [see Eqs. (2) and(3)]. However, in the absence of a definitive model specific to the fluid/solid characteristics of interest that encompasses all of the functionalities and phenomena, a flush velocity must not only exceed the corresponding critical velocity for the same entering fluid at a given particle concentration, it must account for potential transient solids concentrations.

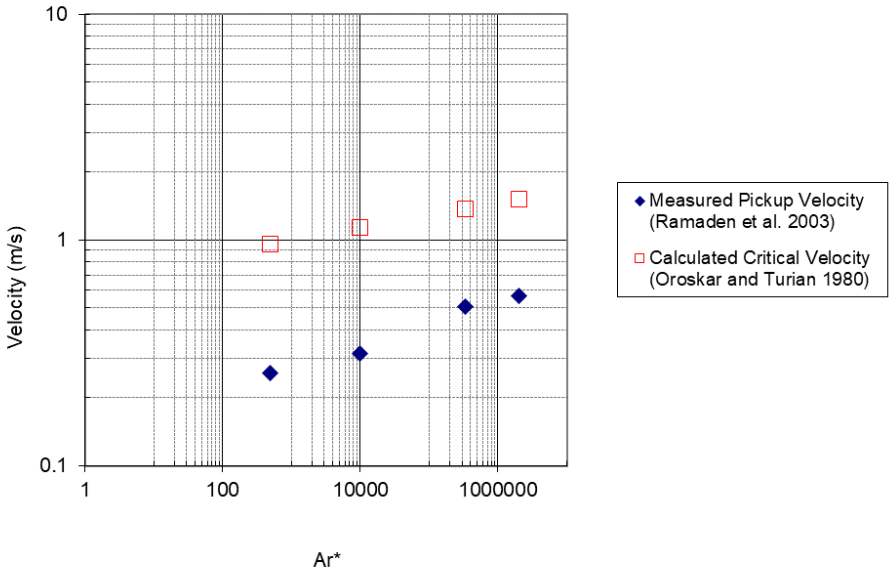


Figure 4. Comparison of calculated critical velocity and pickup velocity for Ramadan et al. (2003) tests

The question “by how much does the flush velocity need to exceed the critical velocity?” thus is more complex than a “set” value. What is the applied stress, i.e., the flush velocity for a given fluid, required to achieve a resuspension rate at which effective flushing is accomplished (e.g., effective flushing in that flush duration/volume is minimized so that system fluid addition is minimized, flushes are conducted with flow rate controls to prevent issues with process piping component configurations, etc.)? What is the effect of particle properties (and sediment conditions) on this flush velocity? Is this flush velocity sufficient to maintain suspension as the particle concentration in the flush fluid is increased? How are the flush and critical deposition velocities impacted by suspended material altering the suspending fluid characteristics?

Addressing these questions quantitatively is beyond the scope of this current work. As previously emphasized, the calculations presented herein do not provide operational requirements, they provide a scoping basis for understanding the potential operational significance of solids precipitation in the AP-106 to WTP LAW feed pipeline. Therefore, a simple method to account for the difference in flush and deposition velocities dependent on particle characteristics at an equivalent concentration is described, and the effect of concentration is addressed via the critical velocity.

As exemplified, direct comparison of flow velocities from the particle pickup model of Rabinovich and Kalman (2007) and the critical velocity model of Oroskar and Turian (1980) is rendered meaningless by the effect of solids concentration. To consider the extent to which the flush velocity may need to exceed the critical velocity, the literature was briefly reviewed for critical deposition velocity models for horizontal pipe liquid transport with negligible (i.e., particle basis) solids concentrations to enable consistent-basis use of the particle pickup model of Rabinovich and Kalman (2007). In the absence of an

identified model, the particle transportation (critical deposition) and resuspension (flush) velocities of Schwuger (1996), shown in Figure 1 of this report, are revisited.

As described, the Figure 1 velocities as a function of particle size are for monodispersed particles at a constant particle density of 2.65 g/mL in hydraulic open channel flow. The data were compiled and originally presented by Hjulström (1935). For application of the Figure 1 results to the current investigation, challenges include open channel versus pipe flow, liquid property variations, single particle versus varied and appreciable concentrations, varied particle density, and polydisperse particle sizes. To address these differences, it is again important to keep in mind that the calculations presented herein do not provide operational requirements. Rather, the calculations provide a scoping basis for understanding the potential operational significance of solids precipitation in the AP-106 to WTP LAW feed pipeline.

With respect to open channel vs. pipe flow, the similarities for flush and critical deposition velocities, and the ratios thereof, either directly from or inferred from Zenz (1964), Nguyen et al. (2016), Poloski et al. (2009), and Rabinovich and Kalman (2007) presented above suggest sufficient basis for application to the current work. The agreement of the Rabinovich and Kalman (2007) model, which includes both channel and pipe flow, with Schwuger (1996), as discussed below, also provides a favorable indication for scoping use. As previously noted, the Rabinovich and Kalman (2007) model, Eq. (3), has some uniqueness with respect to other literature, but they argue that, “As expected, the pickup velocity results of particles by liquids overlap the results in gas–particle systems at Zone I” (as previously quoted). Further, the liquid data set Rabinovich and Kalman (2007) used to develop Eq. (2) does include a limited number of tests with oil as the liquid phase. Again, for the current scoping evaluation, these bases are used as sufficient. The varied particle density and size are also addressed. The varied solid concentration is considered via the Oroskar and Turian (1980) critical deposition velocity model [Eq. (2)] as described in Section 4.2.

Calculated results for the particle pickup velocity [via Eq. (3)] of the potential precipitated solids in the AP-106 to WTP LAW feed pipeline (Section 3.0) are superimposed on Figure 1 and presented in Figure 5. Results at the densities specified in Section 3.0 as well as at the constant density of Schwuger (1996) (2.65 g/mL) are shown to have favorable agreement for particle sizes larger than the $Na_3FSO_4$ (kogarkoite) at 176 µm (0.176 mm). As noted previously, the increase in the erosion (resuspension) velocity below ~200 µm is attributed to cohesive effects which, although likely for some of the precipitates (see Section 3.0 with respect to gels), are not evaluated in this current work.

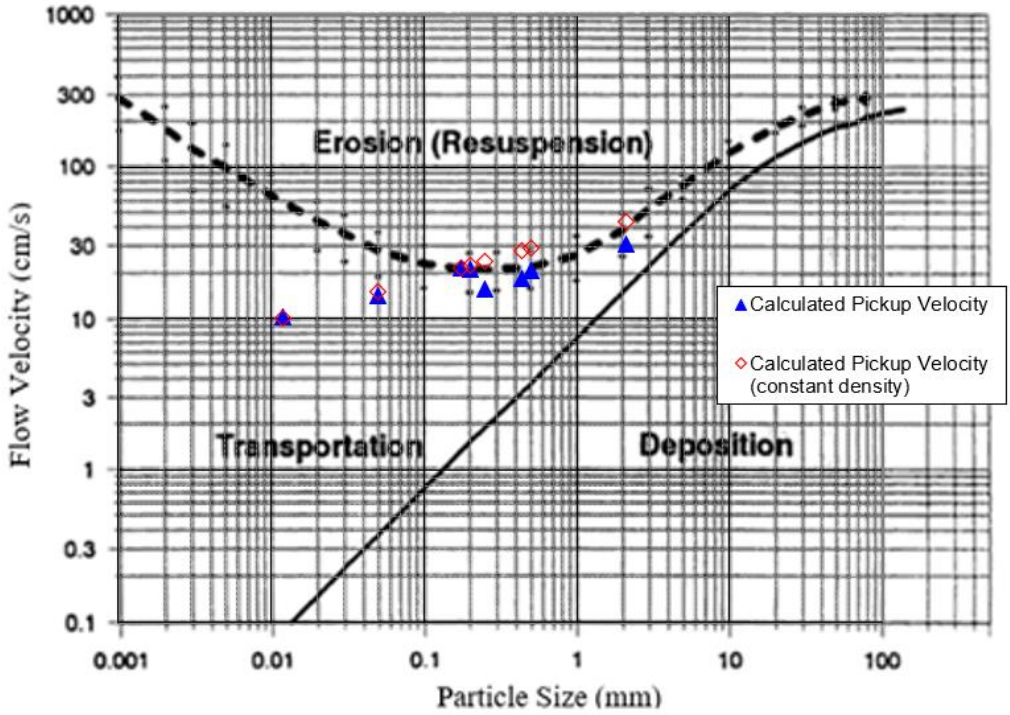


Figure 5. Particle transportation (critical deposition) and resuspension (flush) velocities as a function of particle size in water (from Schwuger 1996) with calculated single particle pickup (flush) velocities.

With the effects of flow configuration, particle size, and particle density in relative "agreement," the ratio of the particle resuspension (flush) and transportation (critical deposition) velocities of Schwuger (1996) are provided in Figure 6, as inferred from Figure 5, for the potential precipitated particles of Section 3.0. Also included is the ratio at a particle size of 10,000 µm (10 mm) (red diamond in Figure 6). Particle density is not accounted-for (see relatively minor variation effect for the particles of interest herein in Figure 5). Depending on particle size, the flush-to-critical-deposition velocity ratio varies from over 16 at 176 µm to 2.8 at 2100 µm [$Na_7F(PO_4)_2 \cdot 19H_2O$ (natrophosphate) at in-tank maximum primary particle size]. Favorable comparison to the experimentally observed ratio from Zenz (1964), as previously presented, is shown for the larger particles.

The velocity ratios of Figure 6 are thus subsequently employed to support the scoping basis for the understanding of the potential operational significance of solids precipitation in the AP-106 to WTP LAW feed pipeline. Using the velocity ratio from the critical deposition velocity results in the solids concentration effects in the flow being represented in some sense, but does not account for an erosion rate. No quantitative understanding for the effect of the resultant flush velocities for the rate of erosion, i.e., see Figure 3 and related discussion, is pursued for the current work given the lack of erosion rate data for Hanford waste. However, given that the resultant flushing velocities are greater than the single particle pickup velocity as shown in Figure 5, and that a solids concentration in the flow will be represented through the ratio to the critical deposition velocity, it can be qualitatively noted that the erosion rate will be greater than the minimum. Understanding the extent of the erosion rate increase requires data specific to the sediment in question (e.g., see discussions provided in Peltier et al. 2012 and Gauglitz et al. 2017).

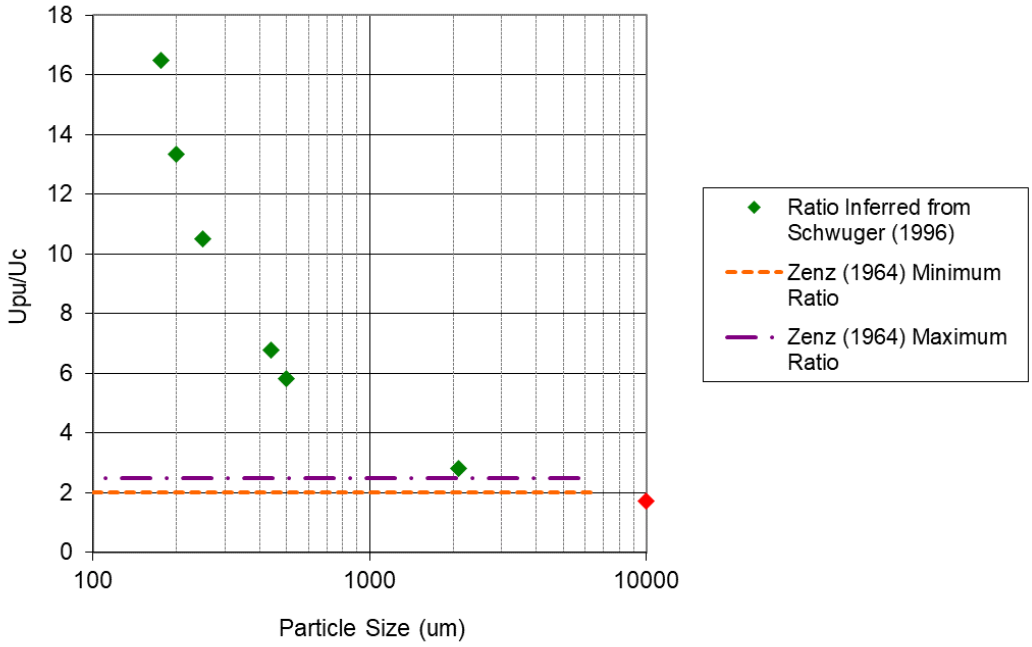


Figure 6. Ratio of flush velocity ($U_{pu}$) to critical deposition velocity ($U_c$) for single particles inferred from Schwuger (1996).

### 4.1.3 Pressure Loss

Simple scoping calculations for the effect of pipeline velocity changes for flushing operations are conducted on a summary[1] of the transfer line parameters based on Dixon (2019). The pressure drop calculations are not intended to represent the actual pressure loss, but instead are approximations made to illustrate the effect of the velocity changes. Application of Bernoulli's equation for the pressure loss ($\Delta P$) roughly accounting solely for pipe length ($L$) and elevation change ($\Delta z$) is conducted as

$$\Delta P = \rho g \Delta z + \frac{1}{2}\rho V^2 f \frac{L}{D} \quad (4)$$

where V is the velocity of interest and f is the resistance coefficient. The pipeline parameter values used are presented in Table 4. In this simplified scoping evaluation, liquid densities and viscosities are not adjusted to account for solids interactions.

[1] Wells BE, LA Mahoney, EJ Berglin, CW Enderlin, RM Asmussen, and MS Fountain. 2019. *Flushing Evaluation for the 241-AP-106 to EMF Transfer Pipeline for DFLAW.* Attachment to LTR-OSIF-008, Pacific Northwest National Laboratory, Richland, Washington. This is not a publicly available document.

Table 4. Pipeline parameter values used for scoping pressure loss calculation.

| Parameter | Value (units) | Reference |
|---|---|---|
| Pipe diameter (3-inch Sch 40 stainless steel) | 3.068 (in.) | 2019 DFLAW flushing evaluation[(a)]<br>CRANE Tech Paper No. 410 |
| Pipe absolute roughness | 0.0006 (in.) | Dixon (2019) |
| Pipe length (AP-106 through the EMF low-point drain LAW feed pipeline) | 3,500 (ft) | 2019 DFLAW flushing evaluation |
| Elevation change, transfer | 26 (ft) | 2019 DFLAW flushing evaluation |
| Elevation change, flush | -26 (ft) | 2019 DFLAW flushing evaluation |

(a) Wells BE, LA Mahoney, EJ Berglin, CW Enderlin, RM Asmussen, and MS Fountain. 2019. *Flushing Evaluation for the 241-AP-106 to EMF Transfer Pipeline for DFLAW.* Attachment to LTR-OSIF-008, Pacific Northwest National Laboratory, Richland, Washington. This is not a publicly available document.

## 4.2 Comparison of Calculation Results to Capabilities of the AP-106 to WTP LAW Feed Pipeline

The calculation bases for critical deposition velocity, flush velocity, and pressure drop described in Section 4.1, are applied and results are discussed in comparison to the AP-106 through the EMF low-point drain LAW feed pipeline capabilities. As previously emphasized, the results presented do not provide operational requirements but rather provide a scoping basis for understanding the potential operational significance of solids precipitation in the AP-106 to the EMF low-point drain WTP LAW feed pipeline.

Velocity and pressure results for comparison to the WTP LAW feed pipeline capabilities are calculated for the system flow ranges: 60 to 88 gpm for feed (Dixon 2019), 60 to 88 gpm for flushing.[1] The piping evaluated is 3-inch stainless steel Sch 40 (Dixon 2019). Feed flow evaluations for critical deposition velocity are conducted at the maximum expected liquid density and viscosity in the transfer pipeline (1.285 g/mL, 6.5 cP) specified in Section 3.0. The flush flow evaluations use the liquid density of the EMF condensate/scrubber liquid, 1.00 g/mL at a viscosity of 1 cP from Section 3.0. As noted in Section 3.0, liquids with maximum and minimum density are both pertinent to aluminum hydroxide precipitation, but the minimum-density liquid would not be present at the same time as salt precipitate (because the salt would dissolve). Therefore, given that the Case 2 precipitation assumption yields the largest total precipitated solids composition (see Section 3.0), the maximum liquid density and viscosity are used for the feed flow evaluations even though this result can be nonconservative.

Figure 7 shows the calculated deposition velocities using Eq. (2) for the potential precipitated solids. As specified in Section 4.1, the factor of 1.3 required by TFC-ENG-STD-26 (2019) is applied to the calculated critical deposition velocity results. Two solids concentrations are used. The Maximum Case Total Concentration is the maximum total for the three bounding assumption cases for precipitation described in Section 3.0. From Table 3, the maximum total concentration of precipitated solids is 3.36 vol% for Case 2. This approach of assigning the maximum concentration to each particle, regardless of the actual estimated precipitations, is clearly unphysical, but it is conservatively bounding. Also evaluated is the result for each of the individual constituent's concentrations for Case 2, labeled in Figure 7 as Maximum Case Constituent Concentrations. This result, while being more representative for each constituent, is also unphysical with respect to the transport velocity as the flow condition of interest contains the total solids concentration. The latter approach therefore provides an under-estimate lower bound. These solids concentration approximations exemplify the issue of applying the Oroskar and Turian

[1] Email from RL Hanson, Bechtel, to BE Wells, PNNL, "RE: EMF Process Condensate Transfer to Tanks Farms", 1/13/20.

(1980) model, or any model developed for monodisperse solids, to polydisperse waste solids.[1] For each solids concentration, the particle size is the 14-day maximum from Table 2.

Also included in Figure 7 are the velocities associated with the feed pipeline flow rates of 60 and 88 gpm. Only the kogarkoite (176 µm, 2.65 g/mL) is shown to exceed the pipeline velocity capability of 60 gpm at the maximum total concentration, but 88 gpm is sufficient. To further bound the analysis, the critical deposition velocities for the in-tank maximum particle sizes provided in Table 2 are also calculated. The results are compared to the 14-day particle size result in Figure 8. Again, 88 gpm is shown to be sufficient to transport all of the potential precipitated solids, even for the bounding analysis, but the gibbsite (200 µm vs. 14-day 50 µm, 2.42 g/mL), and $Na_7F(PO_4)_2 \cdot 19H_2O$ (2100 µm vs. 14-day 500 µm, 1.75 g/mL) have calculated critical deposition velocities that exceed the 60-gpm system velocity. Based on the scoping calculations via the methods and conditions specified, operation of the AP-106 to WTP LAW feed pipeline at 60 gpm can result in the deposition of precipitated solids during flowing conditions, but operation at 88 gpm will not.

The pipeline system must not only be capable of delivering the prescribed transport velocities (i.e., flow rates) for slurry transport and particle resuspension, it must be capable of accommodating the pressures that will be generated at the prescribed flow rates. Comparison of the calculated flow velocities presented in Figure 7 to the pipeline pressure limits is made for this assessment. The pipeline maximum pressure limits are provided in Dixon (2019) as 400 psig for the AP06A central pump pit to the ICD-30 location (Tank Farms/WTP transfer lines interface point) (substituted to represent the AP-106 to EMF line evaluated herein), and 150 psig for all WTP piping for ICD-30 interface to LAW receipt vessels LCP-VSL-00001 or LCP-VSL-00002. Within this pipeline, Dixon (2019) calculated the pressure at the pump discharge nozzle in AP-106 to be 100 psig, and the corresponding pressure under flow at ICD-30 to be 58 psig. The pressure drop in this portion of the line is then 100 psig - 58 psig = 42 psig. The details of the system downstream of the ICD-30 location will not be considered and the pressure drop through this portion of the transfer line will be ratioed to the 400-psig system piping pressure limit, which is 9.52 (400/42) [designated in legend of Figure 9 as Dixon (2019) Pressure Differential from AP-106 to EMF Limit]. Ratioing the pressure drop to the pressure limit will allow a simplified comparison to pressure drops calculated via Eq. (4), which only considers head losses associated with elevation change and line length.

[1] An example discussion of the effect of polydisperse solids representing Hanford waste for mobilization in a mixing vessel by fluid jets is provided in Fiskum et al. (2017) based on simulant slurries. An empirical methodology for employing the Oroskar and Turian (1980) model to estimate the critical deposition velocity relative to specific waste feed requirements for polydisperse solids has also been developed in Wells BE and SK Cooley. 2019. *Comparison of Hanford Waste Solids Physical Characteristics to Specific Requirements of the Hanford Tank Waste Treatment and Immobilization Plant Pretreatment Facility Interface Control Document*. PNNL-SA-145785, Pacific Northwest National Laboratory, Richland, Washington.

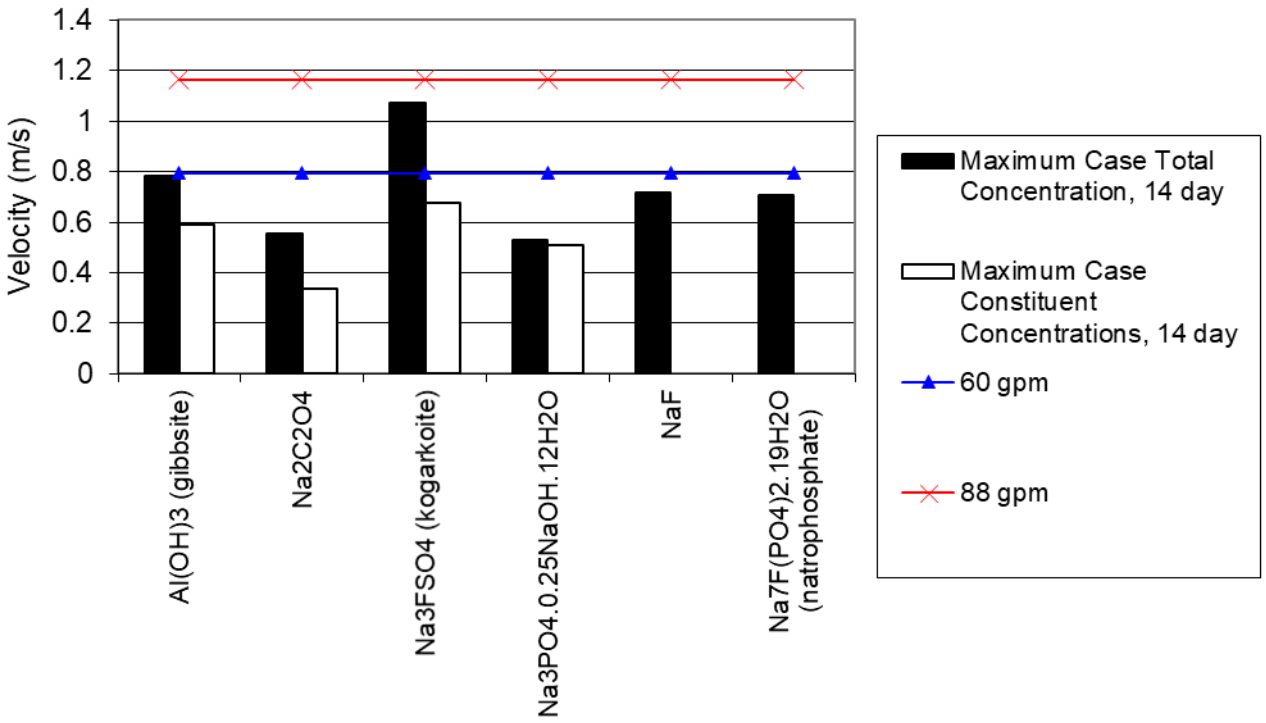


Figure 7. Calculated critical deposition velocities with 14-day particle sizes.

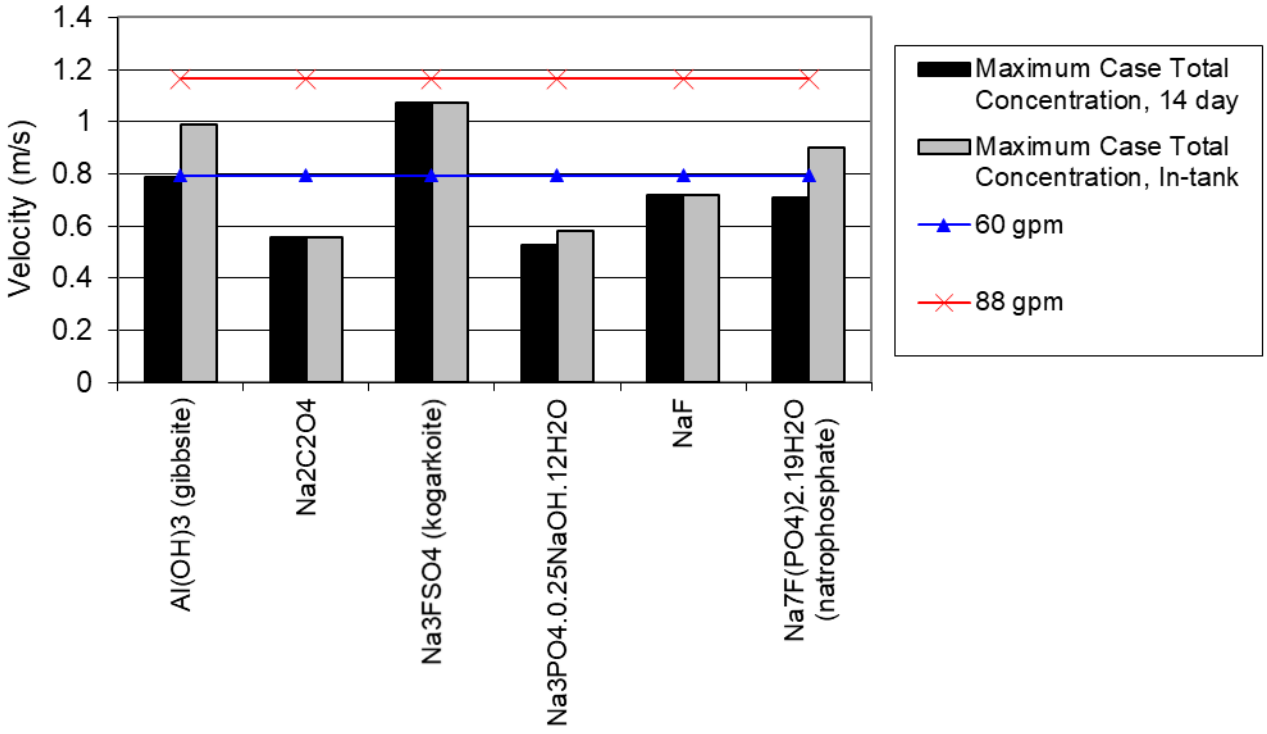


Figure 8. Calculated critical deposition velocities with 14-day and in-tank particle sizes.

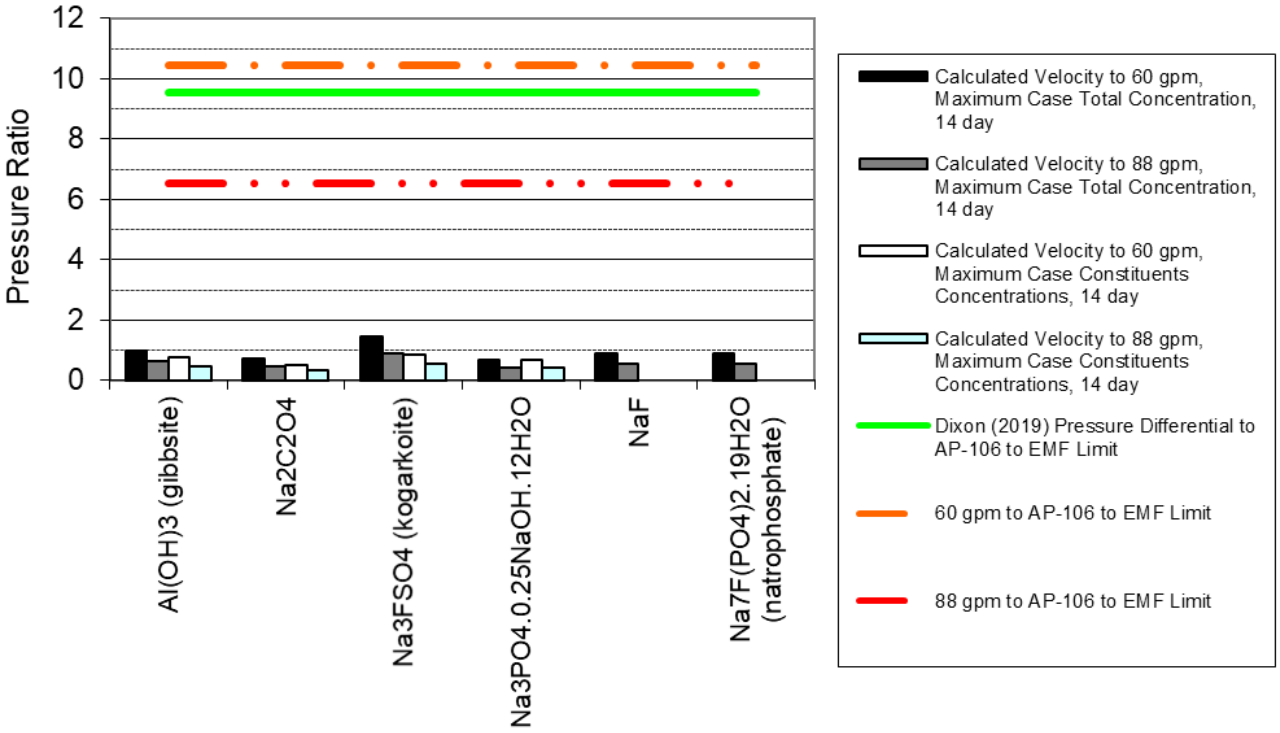


Figure 9. Calculated pressure ratios for critical deposition velocities.

The pressure drops that would occur for 60 and 80 gpm flows of supernatant, calculated via Eq (4), are ratioed to the 400-psig limit and yield values of 10.48 and 6.56, respectively. These values are denoted as 60 gpm and 88 gpm to AP-106 to EMF limit in Figure 9 and comparison to the Dixon (2019) ICD-30 flowing condition to AP-106 to EMF limit value provides a superficial benchmarking of the simple pressure loss calculation of Eq. (4). For assessment of the pressure drops generated by the critical velocities presented in Figure 7, the pressure drops are ratioed to the pressure drops obtained with Eq. (4) resulting for supernatant flows of 60 and 88 gpm. All of the pressure loss ratios for the calculated critical deposition velocities of the potential precipitated solids are, as expected from the Figure 7 results, less than unity with the exception as noted previously for $Na_3FSO_4$ at 60 gpm. While $Na_3FSO_4$ yields the greatest ratio, the pressure limit of the system exceeds the pressure drop (and by comparison the localized pressure generated) resulting from a calculated critical deposition velocity for the most adverse potential precipitated solid.

Based on the critical deposition velocity results presented, one of the potentially precipitated solids may deposit at 60 gpm, but none of them will deposit on the bottom of the transfer pipe invert during flow conditions at 88 gpm. However, under a stopped flow condition, the particles will settle due to their negative buoyancy. The stopped flow condition can occur due to an off-normal event, and also can occur prior to or under incomplete gravity drain. The flushing capabilities of the AP-106 to the EMF low-point drain LAW feed pipeline are therefore evaluated.

The flush velocity-to-critical deposition velocity ratios for single particles inferred from Schwuger (1996) (provided in Figure 6) are shown in Figure 10. Also provided are the available margins (i.e., velocity ratios) between the calculated single particle pickup velocity, Eq. (3), and the 60- and 88-gpm velocities. Finally, the available margin between the calculated critical deposition velocity, Eq. (2), at the maximum total solids concentration, and the 88-gpm velocity is also included. The precipitated solids with no

pickup velocity ratios shown in Figure 10 have particle sizes (refer to Table 2) that are less than either the Rabinovich and Kalman (2007) model modified Archimedes number lower limit or are less than the erosion (resuspension) line minima particle size of Figure 5, and may be more adverse for flushing due to cohesive effects which are not addressed herein.

The purport of Figure 10 is explained using the $Na_3FSO_4$ (deposition of this material can occur at 60 gpm; recall Figure 7) as an example. The ratio of the calculated single particle pickup velocity to 60 gpm is less than unity, and thus, should a $Na_3FSO_4$ particle with the specified characteristics be stationary in a bed of the same particles on the bottom of the pipe invert, a 60-gpm flow with the EMF condensate/scrubber liquid will likely be insufficient to resuspend (flush) the particle. At 88 gpm, however, the $Na_3FSO_4$ ratio is shown as slightly larger than unity, so an 88-gpm flow with the EMF condensate/scrubber liquid will likely be sufficient to resuspend (flush) the particle. A similar result is shown for natrophosphate ($Na_7F(PO_4)_2 \cdot 19H_2O$), and both 60 gpm and 88 gpm are shown as sufficient for gibbsite, $Na_3PO_4 \cdot\cdot 0.25NaOH \cdot\cdot 12H_2O$, and NaF.

Returning to the $Na_3FSO_4$ example, at 88 gpm, the ratio of the calculated critical deposition velocity is less than that for the single particle pickup velocity. This result again demonstrates, in a surrogate manner, the effect of particle concentration, e.g., see Figure 4 discussion. However, insufficient margin is shown between the critical deposition velocity and the available velocity at 88 gpm to attain the Schwuger (1996) ratio: nearly unity in comparison to the Schwuger (1996) ratio of approximately 16.5. Thus, even without taking into account the erosion rate (i.e., see Figure 3 and related discussion; flushing at the single particle pickup velocity will be slow and likely insufficient to maintain suspension as additional particulate is added to the flow), the flushing capabilities of the LAW feed pipeline from AP-106 through the EMF low-point drain are therefore indicated as potentially inadequate for precipitated and settled $Na_3FSO_4$. Potential system inadequacy is also shown for the other particles where the Schwuger (1996) ratios are represented, and the available critical deposition velocity margins, which address concentration in the flow but not flush effectiveness (i.e., erosion rate), are generally shown as less than the typical literature ratio values previously discussed in Section 4.1.2 such as the 2 to 2.5 reported in Zenz (1964) (shown in Figure 5). If cohesive effects were accounted-for (e.g., see discussions of Figure 1, Figure 5, and also Section 3.0), additional challenges may be likely.

Similar outcomes are shown for the calculated results at the maximum case constituent concentrations (i.e., lower concentration than the total; see prior discussion for critical deposition velocity), Figure 11. The $Na_3FSO_4$ ratio for critical deposition velocity increases to slightly more than unity, again far less than the Schwuger (1996) ratio, and nominally a factor of two or more less than other literature values. In addition, for the $Na_3FSO_4$ example, the allowable velocity ratio based on a pressure loss increase to the 400 psig limit (i.e., the flow velocity is determined that provides 400 psig via Eq. (4)) is only approximately 3.3 based on Eq. (4), so the pipeline pressure limit is therefore also indicated as potentially inadequate for effective flushing operations of precipitated solids in comparison to Schwuger (1996).

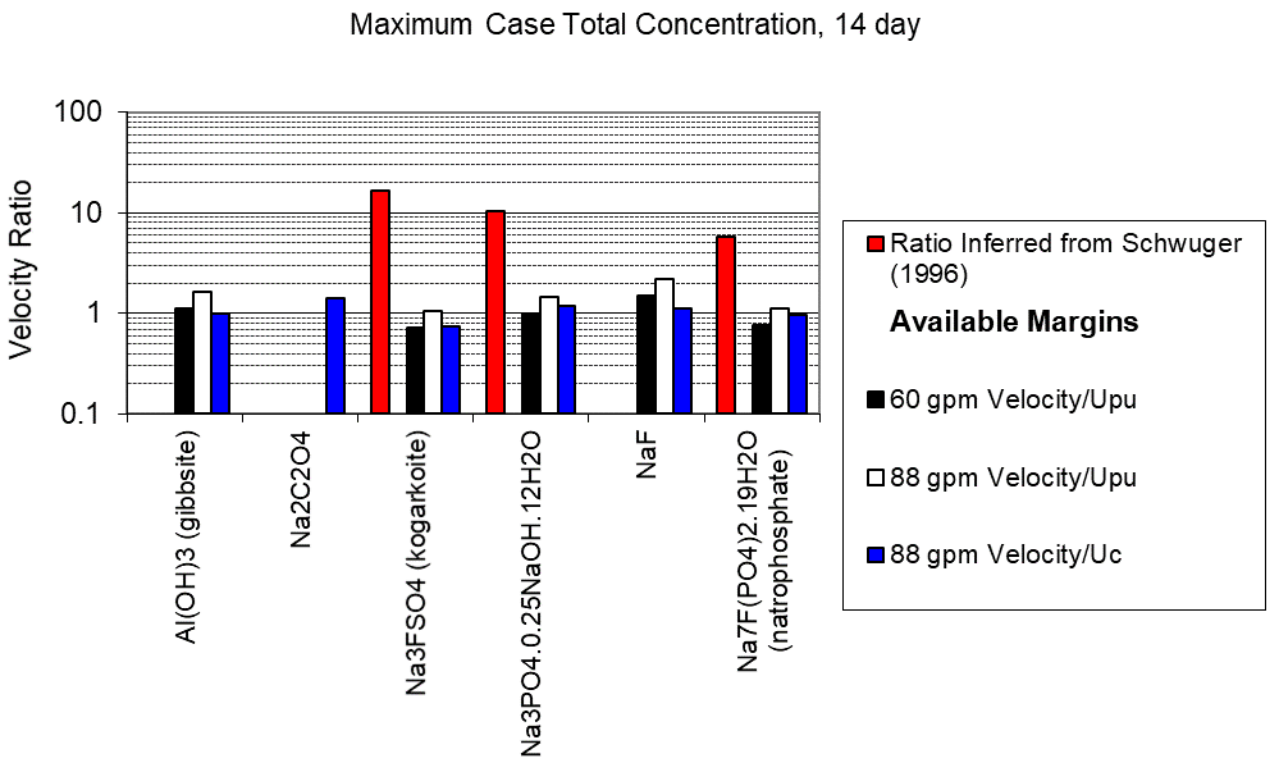


Figure 10. Flush velocity ratios with 14-day particle sizes, maximum total concentration.

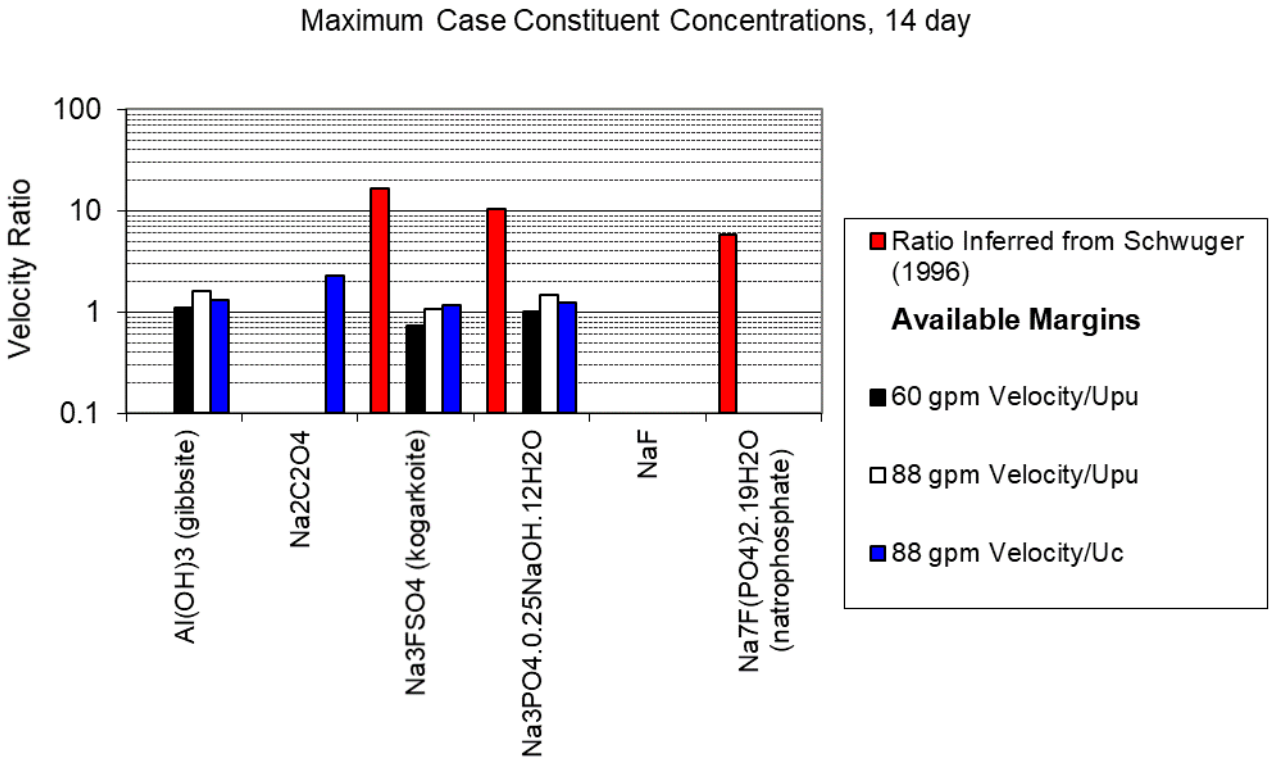


Figure 11. Flush velocity ratios with 14-day particle sizes, maximum constituent concentrations.

The minimum solids concentration of the data set compared to the Oroskar and Turian (1980) model, 0.5 vol%, of Turian et al. (1987) is used to calculate the critical deposition velocity for each of the potential precipitated solids. For reference, the Schappell (2015) treated LAW feed acceptance criteria for the maximum suspended solids concentration is 3.4 wt%, or, for the $Na_3FSO_4$ example with a solid phase density of 2.65 g/mL in water at 1 g/mL, 3.4 wt% is approximately 0.01 vol%. As shown in Figure 12, even at the lower limit of solids concentration for Oroskar and Turian (1980), which can be less than the allowable LAW feed limit, the margin between the calculated critical deposition velocity and the 88-gpm flow is still less than the Schwuger (1996) ratio and typical literature ratios [denoted by the Upper and Lower "ROT" (rule-of-thumb) ratios provided in Figure 12]. The Upper "ROT" Literature Ratio of 4 is approximated, as described in Section 4.1.2, from the Poloski et al. (2009) testing results, which are referenced in TFC-ENG-STD-26 (2019) for a flush velocity basis that "should be sufficient to remove a sediment bed from a 3-inch pipe." TFC-ENG-STD-26 (2019) notes further that, "It is not obvious that this velocity is appropriate for all tank farm operations, and therefore should not be used without consideration of the specific flush application." The evidence therefore again suggests that, even at low solids concentrations, the AP-106 through the EMF low-point drain LAW feed pipeline flushing capabilities are potentially inadequate for effective flushing operations.

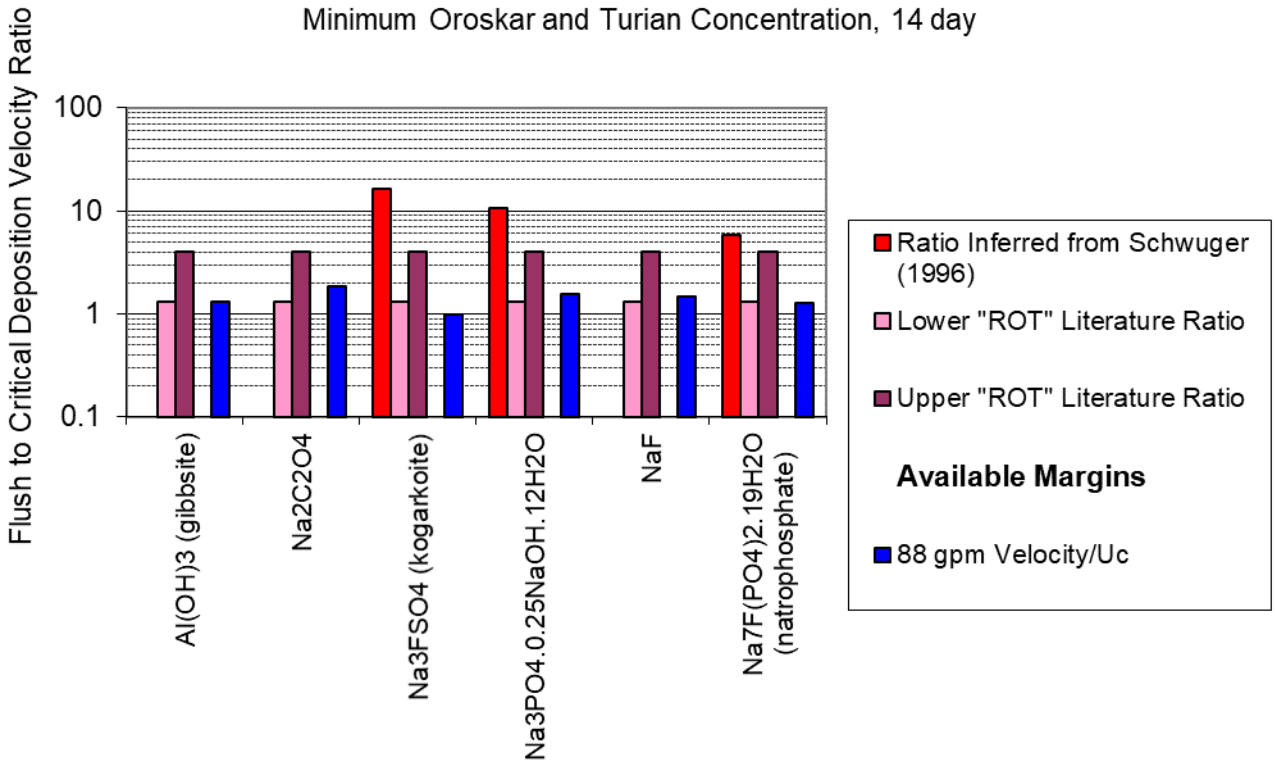


Figure 12. Critical deposition flush velocity ratios with 14-day particle sizes, minimum Oroskar and Turian (1980) concentration.

# 5.0 Summary and Recommendations

The capabilities of the LAW feed pipeline from AP-106 through the EMF low-point drain have been evaluated for the transfer and flushing of potential precipitated solids. The results presented do not provide operational requirements, but rather provide a scoping basis for understanding the potential operational significance of solids precipitation in the pipeline.

Operational experience at Hanford has shown that solids precipitation occurs during processing operations from dilute Hanford liquids. The salt solids that are most likely to precipitate from the LAW feeds during cooling, evaporation, or mixing are NaF (sodium fluoride), $Na_7F(PO_4)_2 \cdot 19H_2O$ (natrophosphate, or sodium fluoride phosphate), $Na_3PO_4 \cdot 0.25NaOH \cdot 12H_2O$ (sodium phosphate dodecahydrate), $Na_3FSO_4$ (kogarkoite, or sodium fluoride sulfate), $Na_2CO_3 \cdot H_2O$ (thermonatrite), $Na_2C_2O_4$ (sodium oxalate), or $NaNO_3$ (sodium nitrate). Aluminum hydroxide (gibbsite), $Al(OH)_3$, is also a potential precipitate from dissolved aluminum at the hydroxide concentrations present in the streams of concern. The particle densities of these potential precipitates are estimated to range from 1.62 to 2.78 g/mL, with a spherical particle size range of 8 to 2100 µm depending upon the constituent.

Application of the TFC-ENG-STD-26 (2019) required method to calculate the critical deposition velocity at conservatively bounding estimates for the solids concentrations demonstrates that one of the potentially precipitated solids may deposit on the bottom of the transfer pipe invert at the lower LAW feed pipeline flow rate of 60 gpm, but that none of them are likely to deposit at the upper LAW feed pipeline flow rate of 88 gpm. In addition, the system pressure limit for the LAW feed pipeline from AP-106 through the EMF low-point drain (400 psig) likely exceeds any pressure loss at a calculated critical deposition velocity even for the most adverse potential precipitated solid based on simplified assessment for line lengths and elevation change.

However, waste transfer lines from the ILST (i.e., AP-106) to the WTP LAW Facility must have the capability of being flushed to prevent accumulation of solids and to mitigate corrosion concerns (Wagnon 2018). The flow capabilities of the LAW feed pipeline from AP-106 through the EMF low-point drain appear, based on the available literature, to be potentially inadequate for effective flushing operations even at solids concentrations below the maximum specified for LAW feed.[1] Thus, solids accumulation resulting from flow stoppage over multiple transfers may be an issue, and eventual line plugging may occur. This analysis does not address any cohesive solids effects, which can be expected for certain precipitates, so further inadequacies and challenges may potentially be realized.

It is further emphasized that, relative to the statement in TFC-ENG-STD-26 (2019) that "[t]here is currently no accepted method to predict the transfer velocity required to re-suspend particles from a sediment bed in a waste transfer line," the identification of the required flush velocity can be substantially complex, and issues presented by solids concentrations can be exacerbated by transients in flow characteristics and process piping component configurations. Not only must a flushing operation be conducted at a velocity that suspends single particles (to be effective, the erosion rate of the settled material must be higher than single particle removal, which, among other issues, would require large flush volumes), the flush velocity must also be sufficient to maintain suspension as the particle concentration in

[1] This analysis focused on precipitated solids for DFLAW. However, given that the particle properties of the potential precipitated solids can have similar particle sizes but lower densities than undissolved solids associated with Hanford high-level waste, the scoping results suggest similar considerations should be made for flushing operations in pipelines that are used for process streams with insoluble solids, especially with respect to the requirements of TFC-ENG-STD-26 (2019).

the flow increases as the flow moves downstream. In contrast, therefore, while the critical deposition velocity can be related to the inflow stream, an effective flushing velocity must not only account for sediment erosion rate and exceed the corresponding critical velocity for the same entering fluid at a given particle concentration, it must account for the total volume of material deposited and transient solids concentrations occurring during the resuspension process.

The scoping calculations, which show that the flow capabilities of the LAW feed pipeline from AP-106 through the EMF low-point drain are potentially inadequate for effective flushing operations, are based on the available literature, and they are subject to uncertainty relative to application to Hanford waste. To confirm these scoping calculations, it is recommended that prototypic laboratory pipeline simulant testing be conducted to substantiate the technical basis for the LAW feed flushing operations. The initial testing objective must be to confirm the scoping calculations, and thereby inform, not resolve, the referenced gap in TFC-ENG-STD-26 (2019) that "[t]here is currently no accepted method to predict the transfer velocity required to re-suspend particles from a sediment bed in a waste transfer line." Upon verification of the scoping calculation results, either effective flushing operations to remove solids should be developed or alternate feed or flushing methods that mitigate the potential for accumulation of precipitated solids must be employed. For example, with respect to concentrated supernatant liquids and soluble solids, TFC-ENG-STD-26 (2019) states that "it is possible for the solids to precipitate during waste transfers, accumulate in the waste transfer line, and start to plug the line. A flush of the waste transfer line will typically dissolve any of these solids." Thus, one operational alternative for flushing would be to use heated flush fluid and increase contact times to re-dissolve any precipitates rather than mobilizing them.

# 6.0 References

ASME. 2000. *Quality Assurance Requirements for Nuclear Facility Applications*. NQA-1-2000, The American Society of Mechanical Engineers, New York, New York.

ASME. 2008. *Quality Assurance Requirements for Nuclear Facility Applications*. NQA-1-2008, The American Society of Mechanical Engineers, New York, New York.

ASME. 2009. *Addenda to ASME NQA-1-2008 Quality Assurance Requirements for Nuclear Facility Applications*. NQA-1a-2009, The American Society of Mechanical Engineers, New York, New York.

Bagnold RA. 1941. "The Physics of Blown Sand and Desert Dunes," SBN 412 10270 6/66. Chapman and Hall, London.

Bolling SD, TM Ely, JS Lachut, and ME LaMothe. 2017. *Solid Phase Characterization of Tank AP-107.* RPP-RPT-60365. Washington River Protection Solutions, LLC, Richland, Washington.

CRC. 1976. *Handbook of Chemistry and Physics, 56th Ed*. CRC Press, Inc., Cleveland, Ohio.

CRANE® Co. 1976. *Flow of Fluids Through Valves, Fittings, and Pipe.* Tech Paper No. 410. Fifteenth printing. CRANE Co. Chicago, Illinois.

Cree LH, CC Groves, DL Herting, JE Meacham, and JG Reynolds. 2017. *Evaluation of Risks to the DFLAW Mission from Solids in East Area Double-Shell Tanks*. RPP-RPT-59586, Rev. 0. Washington River Protection Solutions, LLC, Richland, Washington.

Cree LH, CR Kimura, VC Nguyen, SN Randall, and BM Tardiff. 2019. *River Protection Project Integrated Flowsheet*. RPP-RPT-57991, Rev. 3 (24590-WTP-RPT-MGT-14-023, Rev. 3). Washington River Protection Solutions, LLC, Richland, Washington.

Daniel RC, AJL Fuher, and MS Fountain. 2018. *A Composition-Based Approach for Predicting Hanford Tank Waste Liquid Viscosity*. PNNL-27475, Rev. 0, (RPT-OSIF-001, Rev. 0). Pacific Northwest National Laboratory, Richland, Washington.

Dixon KW. 2019. *AP Farm to Waste Treatment Plant Low Activity Waste Facility Hydraulic Transient Analysis*. RPP-CALC-62531, Rev. 0. Washington River Protection Solutions, LLC, Richland, Washington.

Fiskum SA, CA Burns, NL Canfield, RA Daniel, JA Fort, PA Gauglitz, WL Kuhn, DT Linn, RA Peterson, MR Smoot, BE Wells, and ST Yokuda. 2017. *Standard High Solids Vessel Design Newtonian Simulant Qualification*. PNNL-26103, Rev. 0; WTP-RPT-245, Rev. 0. Pacific Northwest National Laboratory, Richland, Washington.

Gauglitz PA, BE Wells, EJ Berglin, and LA Mahoney. 2017. *Evaluation of A-105 Waste Properties and Potential Simulants for Confined Sluicing Testing*. PNNL-26206. Pacific Northwest National Laboratory, Richland, Washington.

Herting DL, GA Cooke, and RW Warrant. 2002. *Identification of Solid Phases in Saltcake from Hanford Site Waste Tanks.* HNF-11585, Rev. 0. Fluor Hanford, Richland, Washington.

Hjulström F. 1935. *Studies of the Morphological Activity of Rivers as Illustrated by the River Fyris*. Inaugural Dissertation. Uppsala. Almqvist & Wiksells Boktryckeri-A.-B.

Julien PY. 1998. *Erosion and Sedimentation.* Cambridge University Press, Cambridge, United Kingdom.

Lee KP, BE Wells, PA Gauglitz, and RA Sexton. 2012. *Waste Feed Delivery Mixing and Sampling Program Simulant Definition for Tank Farm Performance Testing*. RPP-PLAN-51625, Rev. 0. Washington River Protection Solutions LLC, Richland, Washington.

Mahoney LA and RL Russell. 2006. *Tank 241-S-109 Saltcake Simulant Development and Testing*. PNNL-15699. Pacific Northwest National Laboratory, Richland, Washington.

Mantz PA. 1977. "Incipient Transport of Fine Grains and Flakes by Fluids - Extended Shields Diagram." *Journal of the Hydraulics Division, Proceedings of the American Society of Civil Engineers* 103(6):601-615.

Meacham JE, SJ Harrington, JS Rodriguez, VC Nguyen, JG Reynolds, BE Wells, GF Piepel, SK Cooley, CW Enderlin, DR Rector, J Chun, A Heredia-Langner, and RF Gimpel. 2012. *One System Evaluation of Waste Transferred to the Waste Treatment Plant*. RPP-RPT-51652, Rev. 0. Washington River Protection Solutions, LLC, Richland, Washington.

Nguyen VC, MS Fountain, CW Enderlin, AJL Fuher, and LF Pease. 2016. *One System River Protection Project Integrated Flowsheet – Slurry Waste Transfer Line Flushing Study*. RPP-RPT-59600, Rev. 0. Washington River Protection Solutions, LLC, Richland, Washington.

Oroskar AR and RM Turian. 1980. "The Critical Velocity in Pipeline Flow of Slurries." *AIChE Journal* 26(4): 550-558.

Peltier J, BE Wells, and DR Rector. 2012. *Non-Newtonian Proof of Concept Scoping Test Report*. 24590-WTP-RPT-ENG-11-164, Rev. 0. River Protection Project, Waste Treatment Plant, Richland, Washington.

Poloski AP, ML Bonebrake, AM Casella, MD Johnson, PJ MacFarlan, JJ Toth, HE Adkins, J Chun, KM Denslow, ML Luna, and JM Tingey. 2009. *Deposition Velocities of Non-Newtonian Slurries in Pipelines: Complex Simulant Testing*. PNNL-18316; WTP-RPT-189, Rev. 0. Pacific Northwest National Laboratory, Richland, Washington.

Rabinovich E and H Kalman. 2011. "Threshold velocities of particle-fluid flows in horizontal pipes and ducts: literature review." *Reviews in Chemical Engineering* 27:215-239.

Rabinovich E and H Kalman. 2007. "Pickup, critical and wind threshold velocities of particles." *Powder Technology* 176:9-17.

Ramadan A, P Skalle, and ST Johansen. 2003. "A Mechanistic Model to Determine the Critical Flow Velocity Required to Initiate the Movement of Spherical Bed Particles in Inclined Channels." *Chemical Engineering Science* 58:2153–2163.

Reynolds JG. 2017. *The Solubility of Sodium Carbonate Monohydrate (Thermonatrite) In Hanford Waste Between 5 and 6 M Sodium Concentration*. RPP-RPT-60538, Rev. 0. Washington River Protection Solutions, LLC, Richland, Washington.

Reynolds JG. 2018. “Salt Solubilities in Aqueous Solutions of $NaNO_3$, $NaNO_2$, NaCl, and NaOH: A Hofmeister-like Series for Understanding Alkaline Nuclear Waste.” *ACS Omega* 3:15149-15157.

Reynolds J and D Herting. 2016. “Crystallization of Sodium Phosphate Dodecahydrate and Re-crystallization to Natrophosphate in Simulated Hanford Nuclear Waste.” 2016 Waste Management Symposia, March 6-10, 2016, Phoenix, Arizona.

Reynolds JG and DA Reynolds. 2010. “A Modern Interpretation of the Barney Diagram for Aluminum Solubility in Tank Waste.” 2010 Waste Management Symposia, March 7-11, 2010, Phoenix, Arizona.

Schappell B. 2015. *ICD 30 – Interface Control Document for Direct LAW Feed*. 24590-WTP-ICD-MG-01-030, Rev. 0. Bechtel National, Inc., River Protection Project Waste Treatment and Immobilization Plant, Richland, Washington.

Schwuger MJ (ed.). 1996. *Detergents in the Environment*. ISBN 0-8247-9396-X, Marcel Dekker, Inc., New York.

TFC-ENG-STD-26. 2019. *Waste Transfer, Dilution, and Flushing Requirements*. Rev. C-7. Washington River Protection Solutions, LLC, Richland, Washington.

Turian RM, F-L Hsu, and T-W Ma. 1987. “Estimation of the Critical Velocity in Pipeline Flow of Slurries.” *Powder Technology* 51:35-47.

Vanoni AA (ed.). 1975. *Sedimentation Engineering, the ASCE Task Committee for the Preparation of the Manual on Sedimentation of the Sedimentation Committee of the Hydraulic Division*. The American Society of Civil Engineers, New York.

Wagnon TJ. 2018. *Direct Feed Low Activity Waste Feed Transfer Line Flushing Evaluation*. RPP-RPT-60915, Rev. 1. Washington River Protection Solutions, LLC, Richland, Washington.

Wells BE, DE Kurath, LA Mahoney, Y Onishi, JL Huckaby, SK Cooley, CA Burns, EC Buck, JM Tingey, RC Daniel, and KK Anderson. 2011. *Hanford Waste Physical and Rheological Properties: Data and Gaps*. PNNL-20646; EMSP-RPT-006. Pacific Northwest National Laboratory, Richland, Washington.

Wells BE, CW Enderlin, PA Gauglitz, and RA Peterson. 2009. *Assessment of Jet Erosion for Potential Post-Retrieval K-Basin Settled Sludge*. PNNL-18831. Pacific Northwest National Laboratory, Richland, Washington.

Wells BE, MA Knight, EC Buck, RC Daniel, PA Meyer, JM Tingey, WS Callaway III, ME Johnson, DJ Washenfelder, MN Hall, SL Thomson, SK Cooley, LA Mahoney, AP Poloski, GA Cooke, MG Thien, JJ Davis, GL Smith, and Y Onishi. 2007. *Estimate of Hanford Waste Insoluble Solid Particle Size and Density Distribution*. PNWD-3824; WTP-RPT-153, Rev. 0. Battelle – Pacific Northwest Division, Richland, Washington.

Zenz FA. 1964. “Conveyability of materials of mixed particle size.” *Industrial &Engineering Chemistry Fundamentals* 3(1):65-75.

# Distribution List

All distribution of the current report will be made electronically.

Washington River Protection Solutions
- Conner, JM
- Cree, LH
- Gallaher, BN
- Meacham, JE
- Reynolds, JG
- Vitali, JR
- Wagnon, TJ
- WRPS Documents (TOCVND@rl.gov)

Pacific Northwest National Laboratory
- Arm, ST
- Bottenus, CLH
- Enderlin, CW
- Fountain, MS
- Mahoney, LA
- Peeler, DK
- Wells, BE
- Project File
- Information Release

# Pacific Northwest National Laboratory

902 Battelle Boulevard
P.O. Box 999
Richland, WA 99354
1-888-375-PNNL (7665)

***www.pnnl.gov***